Marine climate and hydrography of the Coralline Crag (early Pliocene, UK): isotopic evidence from 16 benthic invertebrate taxa

Rebecca M. Vignols [a,1], Annemarie M. Valentine [b,2], Alana G. Finlayson [a,3], Elizabeth M. Harper [a], Bernd R. Schöne [c], Melanie J. Leng [d], Hilary J. Sloane [d], Andrew L.A. Johnson [b,*]

[a] *Department of Earth Sciences, University of Cambridge, Downing Street, Cambridge CB2 3EQ, UK*

[b] *Department of Natural Sciences, College of Life and Natural Sciences, University of Derby, Kedleston Road, Derby DE22 1GB, UK*

[c] *Institute of Geosciences, University of Mainz, Johann-Joachim-Becher-Weg 21, 55128 Mainz, Germany*

[d] *NERC Isotope Geoscience Facilities, British Geological Survey, Nicker Hill, Keyworth NG12 5GG, UK*

Current addresses.

[1] *British Antarctic Survey, High Cross, Madingley Road, Cambridge CB3 0ET, UK*

[2] *Student Advice and Support Services, Loughborough University, Loughborough LE11 3TU, UK*

[3] *Oil & Gas Authority, 48 Huntly Street, Aberdeen AB10 1SH, UK*

[*] Corresponding author.

Email address: A.L.A.Johnson@derby.ac.uk (A.L.A. Johnson)

Keywords: Coralline Crag, Pliocene, Paleotemperature, Oxygen isotope thermometry, Uniformitarianism

ABSTRACT

The taxonomic composition of the biota of the Coralline Crag Formation (early Pliocene, eastern England) provides conflicting evidence of seawater temperature during deposition, some taxa indicating cool temperate conditions by analogy with modern representatives or relatives, others warm temperate to subtropical/tropical conditions. Previous isotopic ($\delta^{18}O$) evidence of seasonal seafloor temperatures from serial ontogenetic sampling of bivalve mollusk shells indicated cool temperate winter (< 10 °C) and/or summer (< 20 °C) conditions but was limited to nine profiles from two species, one ranging into and one occurring exclusively in cool temperate settings at present. We supplement these results with six further profiles from the species concerned and supply seven more from three other taxa (two supposedly indicative of warm waters) to provide an expanded and more balanced database. We also supply isotopic temperature estimates from 81 spot and whole-shell samples from these five taxa and 11 others, encompassing 'warm', 'cool' and 'eurythermal' forms by analogy with modern representatives or relatives. Preservation tests show no shell alteration. Subject to reasonable assumptions about water $\delta^{18}O$, the shell $\delta^{18}O$ data either strongly indicate or are at least consistent with cool temperate seafloor conditions. The subtropical/tropical conditions suggested by the presence of the bryozoan *Metrarabdotos* did not exist. Microgrowth-increment and $\delta^{13}C$ evidence indicate summer water-column stratification during deposition of the Ramsholt Member, unlike in the adjacent southern North Sea at present (well mixed due to shallow depth and strong tidal currents). Summer maximum surface temperature was probably about 5 °C above seafloor temperature and thus often slightly higher than now (17–19 °C rather than 16–17 °C), but only sometimes in the warm temperate range. Winter minimum surface temperature was below 10 °C and possibly

the same as at present (6–7 °C). An expanded surface temperature range compared to now may reflect withdrawal of oceanic heat supply in conjunction with higher global temperature.

1. Introduction

The Coralline Crag Formation is an early Pliocene marine unit up to 20 m thick occurring in Suffolk, East Anglia, eastern England. Although actual exposures are fairly limited in number, it has an almost continuous onshore outcrop stretching some 25 km south-west from the coastal town of Aldeburgh (Fig. 1), and extends 14 km north-east from there under the southern North Sea (Balson, 1992). Outliers at Ramsholt, Sutton Knoll (also known as Rockhall Wood) and Tattingstone (now submerged beneath a reservoir) extend the area of occurrence of the formation 27 km west-south-west of the main onshore outcrop. The unit is typically a fine–medium sand, strongly bioturbated and with a mud admixture of up to 24% in the Ramsholt Member, but generally less bioturbated and with a lower mud content in the overlying Sudbourne and Aldeburgh members (Balson et al., 1993); the calcium carbonate content is high throughout (usually 60–70%; Balson et al., 1993). Unconformably below and above the Coralline Crag are more extensive marine units with a much lower calcium carbonate content: respectively, the Eocene London Clay Formation and the late Pliocene–early Pleistocene Red Crag Formation.

Following reassignment of the thin (*c*. 4 m) deposit occupying a small area at St Erth, Cornwall, to the Pleistocene (see Fig. 1), the Coralline Crag is the only onshore early Pliocene (Zanclean) deposit in the British Isles. On the opposite side of the southern North Sea, in Belgium and The Netherlands (Fig. 1), there is an extensive, thick and fairly complete sequence of Pliocene marine deposits (Marquet and Herman, 2009), but in Belgium there appears to be a gap corresponding to the time of deposition of the Coralline Crag (De

Schepper et al., 2009; Fig. 2). In The Netherlands, equivalent-aged strata are known only from boreholes so, as an outcropping, moderately well-exposed unit, the Coralline Crag is the best source of information on marine environmental conditions in the southern North Sea Basin for part of the Pliocene. The interval concerned is not represented in the stratigraphic sequence of the northern part of the Atlantic Coastal Plain of the USA (Fig. 2), or farther south (Ward et al., 1991), so the Coralline Crag is important for interpreting early Pliocene environmental history in the wider North Atlantic area. It figures in global reconstructions of sea-surface temperature for part of the late Pliocene (Mid-Piacenzian Warm Period) and in tests of paleoclimate models (including ones used in IPCC projections) tuned to this interval, the data involved (from ostracod-assemblage analysis; see below) being assigned a medium 'confidence level' in recognition of the age discrepancy (Dowsett et al., 2012, 2013).

The Coralline Crag has long been of interest to geologists, partly because of its unusual lithofacies for the Cenozoic of the immediate area, but mainly because of its abundant and diverse biota. Volumetrically, the dominant elements are mollusks and bryozoans (originally thought to be corals, hence the name of the unit; Charlesworth, 1835). The detailed taxonomic composition of the biota was the subject of many studies in the 19th and early 20th centuries (Charlesworth, 1835; Wood, 1848, 1851–61, 1872–74, 1879, 1882; Busk, 1859; Prestwich, 1871; Harmer, 1896, 1914–18, 1920–25), and attention has continued into recent times (e.g., Cadée, 1982; Bishop, 1987, 1994; Balson and Taylor, 1982; Bishop and Hayward, 1989; Wood et al., 1993; Head, 1997, 1998; Long and Zalasiewicz, 2011; Taylor and Taylor, 2012). From the time of the earliest studies there has existed a view that the Coralline Crag represents warm conditions, based on the modern temperature associations of certain taxa ('ecological uniformitarianism'). For example, from the common occurrence of the bryozoans *Cupuladria* and *Metrarabdotos*, restricted today to areas where seafloor temperature does not fall below 12 °C and 16 °C, respectively (Lagaaij, 1963; Cheetham,

1967), a warm temperate to subtropical/tropical marine climate has been inferred (e.g., Taylor and Taylor, 2012). This is in marked contrast to the cool temperate marine climate of the southern North Sea at present (typical winter minimum temperature: 6–7 °C). Temperatures in the cool temperate winter range (< 10 °C) have in fact been inferred from Coralline Crag benthic foraminifers (Murray, 1987), and only just into the warm temperate range from benthic ostracods (Wood et al., 1993). Different groups therefore give different indications. Varying indications are supplied by mollusks, 'Mediterranean' (warm temperate) and 'Arctic' taxa having been recorded in some of the earliest work (Prestwich, 1871) and a similar diversity acknowledged in recent studies (Long and Zalasiewicz, 2011, 2012).

Investigations of temperature by biotic-assemblage analysis have now been supplemented by studies using the isotopic ($\delta^{18}O$) composition of Coralline Crag mollusks. Following initial work on single calcium carbonate samples from shells (e.g., Gladenkov and Pokrovskiy, 1980), research involving serial ontogenetic sampling (isotope sclerochronology) has been undertaken to provide seasonally resolved data. The first results, indicating winter temperatures in the cool temperate range and similar to those at present in the southern North Sea, were thought possibly to be an artefact of alteration in view of the suggestions of higher temperature provided by the large size of microgrowth increments in the bivalve-mollusk subject, *Aequipecten opercularis* (Johnson et al., 2000). The preservation of shell calcite was subsequently determined to be pristine and microgrowth-increment size in this species shown probably to relate to food availability and oxygenation rather than temperature; similar winter temperatures to those previously derived were obtained from further examples of *A. opercularis* (making a total of nine) and from an example of the aragonitic bivalve, *Arctica islandica* (Johnson et al., 2009). Summer temperature estimates from these species were in the cool temperate range for this season (below 20 °C, according to the definition of Hall, 1964) and several degrees lower than the present summer maximum in the southern North

Sea (typically 16–17 °C). For the eight Ramsholt-Member shells, this was thought probably to reflect greater depth (*c*. 50 m) and much weaker tidal currents, enabling water-column stratification in summer—i.e., restriction of summer warming largely to surface waters. This provides a means of reconciling cool temperate summer seafloor temperatures from shell $\delta^{18}O$ with warm temperate (or even subtropical) surface temperatures from assemblages of pelagic dinoflagellates (Head, 1997, 1998). Since dinoflagellates typically encyst in winter they are not sensitive to temperature in that season (Valentine et al., 2011), so their warm temperate signature in this instance is restricted not only to surface temperature but to summer, and hence in no conflict with isotopic evidence of cool temperate winter conditions on the seafloor, and very probably at the surface (Johnson et al., 2009).

The $\delta^{18}O$-based temperatures from *A. opercularis* and *A. islandica* are entirely consistent with the tolerances of modern representatives, the former species extending into and the latter being confined to cool temperate settings. We cannot, however, be sure that they are correct because they were calculated using one of several possible equations, each of which supplies a slightly different result and all of which involve a second 'unknown': water $\delta^{18}O$. Our preferred value for this (+0.1‰), giving the above results, is based on modelling for the specific location and time, but another modelled value (+0.5‰) gives higher temperatures (some just into the warm temperate range for winter but well below the minimum temperature suggested by the presence of the bryozoan *Metrarabdotos*), while the lowest estimate for global average water $\delta^{18}O$ (–0.5‰) gives much lower temperatures (Johnson et al., 2009). The influence of the value chosen for water $\delta^{18}O$ is seen in the preliminary results (temperatures as low as 3.6 °C for a value of –0.35‰) reported by Williams et al. (2009, p. 98) from the $\delta^{18}O$ of additional specimens of *A. islandica* (data considered in full below: *A. islandica* specimens 1, 2 and 5).

While absolute temperature cannot be specified with complete confidence from the $\delta^{18}O$ of skeletal calcium carbonate, this form of data does provide a means of testing whether Coralline Crag taxa lived at different temperatures, as implied by the different temperature associations of modern representatives and close relatives. In order to explain the varying temperature indications from the Coralline Crag, Johnson et al. (2009) adopted the view that the unit must represent a significantly fluctuating marine climate. Although deposition may have taken as little as 200,000 years, this is sufficient to span glacial and inter-glacial stages, and the close juxtaposition of 'warm' and 'cool' taxa could reflect reworking (Williams et al., 2009). Even so, such studies of multiple discrete horizons as have been undertaken (Head, 1997; Long and Zalasiewicz, 2011) have provided little evidence of temporal change in marine climate, and climate change is scarcely credible as an explanation for occurrences in the same bed of articulated examples of both the 'warm' bivalve species *Panopea glycymeris* and the 'cool' species *A. islandica* (Long and Zalasiewicz, 2012). It is conceivable that higher summer surface temperatures than now enabled the coexistence of 'warm' with 'cool' bivalve taxa by providing suitable conditions for the pelagic larvae (cf. Raffi et al., 1985; Long and Zalasiewicz, 2011). However, this is essentially speculative, requiring confirmation that the adults actually lived at the same temperature as those of 'cool' taxa, and that the water column was stratified (i.e., much warmer at the surface) in summer.

In the following, we supplement the existing isotopic temperature data for *A. opercularis* and *A. islandica*, and supply data for 11 further bivalve species, two gastropod mollusk species and a brachiopod species. This set spans 'cool', 'warm' and 'eurythermal' species on the evidence of modern representatives and close relatives, thus allowing us not only to test for predicted temperature differences but also to obtain a representative overview (as far as it was possible to preordain) of Coralline Crag conditions. Limitations in the availability of analytical resources, and the variable or unknown growth rate of species, led us to acquire a

heterogeneous dataset in terms of the temporal resolution of sampling. However, this is sufficient, if used with care, to determine whether species supposedly indicative of different temperature regimes did indeed occupy them, and, with appropriate qualifications, to supply estimates of absolute seafloor temperature. We use $\delta^{13}C$ data (obtained from shell samples alongside $\delta^{18}O$), together with microgrowth-increment data from *A. opercularis*, to test for summer water-column stratification (Johnson et al., 2009, 2017). From the outcome of this test we are able to project summer surface from seafloor temperatures, again with appropriate qualifications. We supply evidence of excellent shell preservation to confirm that the $\delta^{18}O$ and $\delta^{13}C$ values can be accepted as original.

2. Material and methods

2.1. Taxa chosen

The generic and specific taxonomy used in the following, together with information on the geographic ranges of modern representatives and close relatives, derives from a variety of authoritative on-line sources (Encyclopaedia of Life, Marine Bivalve Shells of the British Isles, Marine Life Information Network, Ocean Biogeographic Information System [OBIS], World Register of Marine Species), supplemented by Huber (2010). The taxonomy differs in some respects from that in other recent work on the Pliocene biota of the southern North Sea Basin (Marquet, 2002, 2005; Long and Zalasiewicz, 2011, 2012). However, the identity of the taxa referred to should be clear. Illustrations of some, together with isotopic-sampling traces, are provided in Figure 3.

As 'warm' taxa from the Coralline Crag we chose the bivalves *Cardites squamulosa ampla* (Chavan and Coatman 1943), *Coripia corbis* (Philippi 1836) and *Talochlamys*

multistriata (Poli 1795), the gastropod mollusk *Ringicula buccinea* (Brocchi 1814), and the unusually large brachiopod *Pliothyrina maxima* (Charlesworth 1837). *C. squamulosa ampla* (Fig. 3C) and *C. corbis* are both carditids, a family not represented in the modern North Sea. *C. squamulosa ampla* appears to be extinct, but has a very close modern relative (probably a descendant) in *Cardites antiquatus* (Linnaeus 1758), which is restricted to the Mediterranean (Fig. 3D). *C. corbis* is extant and likewise restricted today to the Mediterranean, as is the pectinid *T. multistriata* (Fig. 3B). Records of the latter from southern Africa are very distant from the main area of occurrence and probably represent a different species. The ringiculid *R. buccinea* (Fig. 3H) and terebratulid *P. maxima* are both extinct. Recent records of close modern relatives of the former are restricted to the Mediterranean, although Jeffreys (1871) did record *Ringicula auriculata* (Ménard de la Groye 1811) from the North Sea. Being representative of an extinct genus, *P. maxima* has no close modern relatives. Other *Pliothyrina* species occur in the Plio-Pleistocene of Italy, suggesting an affinity for warm conditions. No such large brachiopods occur in the modern North Sea.

As 'cool' taxa we chose the bivalves *Arctica islandica* (Linnaeus 1767), *Mya truncata* (Linnaeus 1758), *Glycymeris obovata* (Lamarck 1819), *Astarte gracilis* Goldfuss 1837 and *Astarte omalii* (de la Jonkaire 1823), and the gastropod *Retusa conuloidea* (Wood 1851). Like the arcticid *A. islandica*, the myid *M. truncata* is extant and occurs at present in the North Sea but extends no farther south in the eastern North Atlantic than northern France (northern boundary of warm temperate marine climate; Hall, 1964). The glycymerid *G. obovata* is extinct. The close modern relative *G. glycymeris* (Linnaeus 1758) is absent from the North Sea at present but occurs as far south as northern France. The astartids *A. gracilis* (Fig. 3E) and *A. omalii* are likewise extinct. The close modern relatives *Astarte elliptica* (Brown 1827) and *A. montagui* (Dillwyn 1817) occur essentially around the UK (although not in the southern North Sea) at present, but *A. acuticostata* Friele 1877 is found only in the

northern UK and farther north. The retusid *R. conuloidea* is also extinct. The close modern relatives *R. obtusa* (Montagu 1803) and *R. truncatula* (Bruguière 1792) occur at present in the North Sea, and the former is found elsewhere around the UK and northern France.

As 'eurythermal' taxa we chose the bivalves *Aequipecten opercularis* (Linnaeus 1758), *Palliolum tigerinum* (Müller 1776), *Pecten* aff. *grandis* J. de C. Sowerby 1828, *Lucinoma borealis* (Linnaeus 1767) and *Spisula arcuata* (J. Sowerby 1817). The pectinids *A. opercularis* (Fig. 3A) and *P. tigerinum* are both extant and occur today from Norway (cool temperate marine climate) to the Mediterranean, although the latter is absent or scarce in the southern North Sea. The pectinid *P*. aff. *grandis* is extinct. The close modern relative *Pecten maximus* (Linnaeus 1758) occurs at present from Norway to the Iberian Peninsula but is relatively uncommon in the North Sea. The lucinid *L. borealis* (Fig. 3F) is extant and occurs today from the northern UK to the Mediterranean. The mactrid *S. arcuata* (Fig. 3G) is extinct. The close modern relatives *S. elliptica* (Brown 1827), *S. solida* (Linnaeus 1758) and *S. subtruncata* (da Costa 1778) are mainly known at present from the North Sea, but *S. solida* is recorded from the Mediterranean.

2.2. Specimens used

Specimens (total 83) were selected from pre-existing collections in the Sedgwick Museum, University of Cambridge, UK; Geological Collections, Department of Natural Sciences, University of Derby, UK; Institute of Geosciences, University of Mainz, Germany; or they were collected from the Sutton Knoll site. Wherever possible, we utilised material known to be from the Ramsholt Member, where preservation is generally better (Balson, 1983), but no finer stratigraphic determination was attempted. None of the specimens were definitely from the overlying Sudbourne or Aldeburgh members. Individuals were selected

that visually appeared well preserved, without obvious bioerosion and as whole as possible. Taxon, repository and provenance of specimens, mineralogy of the sampled layer, type of sampling undertaken, sample positions (ontogenetic sampling), laboratory where analysis was conducted, raw isotope data (including $\delta^{13}C$ values from spot and whole-shell samples not plotted herein), and raw microgrowth-increment data from *A. opercularis*, are given in Supplementary Material A.

2.3. Isotopic sampling strategy

Ideally we would have sampled all species ontogenetically, and done so at high temporal resolution through the growth of all individuals selected—this would have enabled detailed comparisons between species and the most precise reconstructions of seasonal temperatures. Quite apart from the large analytical resource required, it would have been technically difficult to achieve high resolution for years of slow growth (e.g., in late ontogeny) and very time-consuming in those species (the majority) without proven annual growth lines, these requiring preliminary sampling in order to determine annual increments from $\delta^{18}O$ profiles. We therefore took a more diverse approach, nevertheless obtaining some ontogenetic data from each of two 'warm' (*C. squamulosa ampla*, *P. maxima*; four and two specimens, respectively), one 'cool' (*A. islandica*; four specimens) and two 'eurythermal' (*A. opercularis*, *L. borealis*; two specimens and one, respectively) taxa.

A. islandica shells exhibit internal growth lines (Fig. 4A, B) which have been proved to represent annual growth breaks (Witbaard, 1997; Witbaard et al., 1997; Schöne et al., 2005a). We could therefore determine at the outset a sample-spacing necessary to achieve a given temporal resolution. Since similar structures in other ecologically equivalent (infaunal) bivalves are known to be annual (Richardson, 2001), we took those in *C. squamulosa ampla*

(Fig. 4C) to have this periodicity. The annual nature of growth lines has been less widely demonstrated in brachiopods so we could not be sure of the periodicity of those seen externally in *P. maxima*. We therefore took samples from the two shells at quite close spatial separation (mean spacings: 1.2 and 1.4 mm) in the hope that this would provide high temporal resolution. In that the profile from one shell showed two full, well-defined $\delta^{18}O$ cycles (13 samples in each; see Fig. 10A), which can only reasonably be ascribed to seasonal temperature variation, this proved to be the case. The formation of external growth lines ('steps' in the shell profile) in *A. opercularis* does not follow a regular periodicity, but growth in this species is known to be quite rapid (Johnson et al., 2009). By taking samples from the two shells at a similar separation (mean spacings: 1.0 and 1.3 mm) to those from *P. maxima* we could therefore anticipate high temporal resolution. This strategy produced profiles showing between one and two well-defined $\delta^{18}O$ cycles (more than 15 samples per cycle in each shell; see Fig. 9A, B), confirming high temporal resolution. Although samples from the single *L. borealis* shell were taken at a comparable separation (mean spacing: 1.1 mm), the interval sampled (12.4–19.7 mm from the origin of growth) did not provide clear evidence of cyclicity (see Fig. 11A). Equivalent growth in the ecologically similar (infaunal) bivalve *A. islandica* occupies 1–2 years (Witbaard et al., 1997) so the temporal resolution of sampling in *L. borealis* was almost certainly lower than for *P. maxima* and *A. opercularis*. The strategy for *A. opercularis* did, however, provide at least some high resolution data from a 'eurythermal' species, and for *P. maxima* from a 'warm' species. We obtained equivalent data from one specimen of the 'cool' species, *A. islandica*, by sampling years 17–25 at 9–17 samples per year, supplementing existing data (Johnson et al., 2009) for year 3 (mean samples per year: $12.5 \pm 2.5, \pm 1\sigma$). Single samples spanning each annual increment were taken over years 4–16, adding a low-resolution record to the data from this shell. Other specimens of *A. islandica* were sampled at intermediate resolution (total of 12 full years; 2–7

samples per year, mean 4.2 ± 1.8), as were specimens of the second 'warm' taxon, *C. squamulosa ampla* (total of 18 full years, 3–8 samples per year, mean 5.1 ± 1.5), assuming that the growth lines used to define years were indeed annual.

The temporal resolution of sampling is likely to impact on the seasonal temperatures determined so, in general, comparisons should only be made between data of the same original resolution, or 'resampled' to provide the same resolution (Wanamaker et al., 2011). However, comparisons between data of different resolution are meaningful where the lower-resolution data provides a more extreme seasonal temperature. Spot samples representing fairly short intervals (no more than a year) are potentially able to yield temperatures outside the seasonal range determined from ontogenetic samples, thus providing a fuller picture of variability. They are also valuable as a check, albeit crude, on the representativeness of the temperatures from ontogenetic samples. Accordingly, we supplemented the ontogenetic profiles (13, from five taxa) with 23 spot samples (similar in size to individual ontogenetic samples) from 19 specimens of the same taxa (eight specimens of *A. opercularis*, four of *L. borealis*, three of *A. islandica*, two each of *C. squamulosa ampla* and *P. maxima*). As a check on whether the ontogenetically sampled species are representative of the Coralline Crag biota as a whole we took a further 30 spot samples from 24 specimens of other 'warm', 'cool' and 'eurythermal' taxa (six specimens of *A. gracilis*, five of *G. obovata*, three each of *A. omalii* and *S. arcuata*; two each of *T. multistriata*, *P. tigerinum* and *M. truncata*, one of *P.* aff. *grandis*), and nine 'whole-shell' (see section 2.7.2) samples of each of *C. corbis* ('warm'), *R. buccinea* ('warm') and *R. conuloidea* ('cool'), the specimens of these three species being too small (< 3 mm) to manipulate for spot sampling. Whole-shell samples have the disadvantage that they incorporate inner-layer material, which may have a non-equilibrium isotopic composition (Hickson et al., 1999), and in our case they were larger than spot samples, possibly representing up to a year given the size of the specimens used.

2.4. Preparation of material for investigation

Material was prepared for investigation (assessment of preservation, detection of annual growth lines, measurement of microgrowth increments, isotopic sampling and analysis) in various ways according to general convention, institutional preference, and the specific focus of the study.

Specimens were initially scrubbed with a nylon brush in water and (where necessary) agitated in an ultrasonic bath to detach sediment and encrusting organisms from the outer surface. Those to be photographed for illustrative purposes or microgrowth-increment measurement (*A. opercularis*) were coated with a sublimate of ammonium chloride to improve the visibility of surface details. All were subsequently rinsed in tap-water and air-dried. Specimens of *C. squamulosa ampla* and *A. islandica* intended for ontogenetic isotopic sampling, together with two more *A. islandica* specimens intended for preservational assessment alone, were encased partly or fully in resin to permit sectioning without risk of shell disintegration. Specimens were then cut with a circular saw perpendicular to the shell surface along the axis of maximum growth. The cross-sections of encased shells (both 'halves') were ground and polished with increasingly fine abrasive papers or powders (down to 1 μm) to remove scratches, followed by rinsing in deionised water and air-drying. Specimens of *A. opercularis*, *L. borealis* and *P. maxima* intended for ontogenetic isotope sampling were not encased and sectioned but those of *A. opercularis* were subjected to an additional procedure (involving bleach and ethanol) for cleaning the exterior (details in Valentine et al., 2011).

Fully encased and sectioned shells were etched in 1‰ hydrochloric acid and used to make acetate-peel replicas of the cut surface for identification of annual growth lines under the

optical microscope (Richardson et al., 1979). In the case of *A. islandica* specimen BRS-AJ1-CC-D1R, which was only encased in resin adjacent to the axis of maximum growth, an acetate peel was not made but the cut surface of one 'half' was stained with Mutvei's solution (Schöne et al., 2005b) to enhance the visibility of internal growth lines under the optical microscope.

The 'half' of fully encased specimens of *C. squamulosa ampla* that had not been used for acetate-peel production was employed to make a petrological thin-section for use in assessment of preservational status by cathodoluminescence (CL). Two specimens of *A. islandica* not intended for ontogenetic isotopic sampling were also treated in this way. Thin-sections were carbon-coated and investigated with a 'cold' cathode instrument built in-house at the University of Cambridge (accelerating potential = 26kV; gun current = 500/700 mA; vacuum = 0.01–0.05 Torr). The 'half' of one specimen of *C. squamulosa ampla* used for peel production, together with an equivalent 'half' of one specimen of *A. islandica*, was re-polished, re-etched and gold-coated for assessment of preservational status in the scanning electron microscope (SEM). SEM investigations were also made of fractured, ultrasonically cleaned and similarly coated specimens of 12 of the 16 species (no specimens of *G. obovata*, *P. tigerinum*, *C. squamulosa ampla* and *M. truncata* were investigated in this way). Two specimens of *C. squamulosa ampla* and one of *S. arcuata* that had undergone nothing more than initial cleaning were used for assessment of preservational status by x-ray diffraction (XRD) analysis. For *C. squamulosa ampla* the fairly large amount of powder required (*c*. 5 mg) was obtained by a combination of drilling and scraping; for the small species *S. arcuata* the entire shell was crushed using a pestle and mortar.

2.5. Assessment of preservation

Shelled organisms exhibit taxon-specific microstructures (e.g., Bieler et al., 2014) which are unlike abiogenic occurrences of the minerals concerned. The appearance of shell material under the SEM can therefore be used to judge whether it is in the original state or altered. Cathodoluminescence is blue in the case of aragonite and orange in calcite; hence, the occurrence of orange luminescence in originally aragonitic material is evidence of alteration. XRD spectra can be used likewise to detect alteration by comparison with calculated spectra for aragonite and calcite.

2.6. Use of growth lines and microgrowth increments

The internal growth lines revealed in *A. islandica* and *C. squamulosa ampla* by sectioning, and taken to be annual, were used to define annual increments, thus allowing samples from cross-sections to be referred to a particular ontogenetic year (numbered by counting from the origin of growth) and for the temporal resolution of sampling to be determined.

The microgrowth increments observable on the outer surface of *A. opercularis* (Fig. 4D) represent intervals in the order of a day (Broom and Mason, 1978). Their size (anatomical height as seen in 2D digital photographs) through ontogeny was measured using the bespoke software Panopea© (2004, Peinl and Schöne) for comparison with the pattern of variation in $\delta^{18}O$. Specimens of *A. opercularis* from well-mixed settings typically show only high-frequency (*c.* monthly), low-amplitude variation in microgrowth-increment size over the span of an annual $\delta^{18}O$ cycle, but superimposed on this in specimens from seasonally stratified settings is typically a low-frequency (*c.* annual), high-amplitude pattern (Johnson et al., 2009, 2017). The microgrowth-increment approach to interpreting hydrographic setting is a useful supplement to the more established technique involving $\delta^{13}C$ (e.g., Arthur et al. 1983; Krantz et al., 1987; Krantz, 1990), which is not infallible (Johnson et al., 2017).

2.7. Isotopic sampling

2.7.1. Ontogenetic sampling

With the exception of the brachiopod *P. maxima*, from which material was extracted from the secondary (inner) layer because of concerns over possible 'vital' effects on isotopic composition in the primary (outer) layer (Carpenter and Lohmann, 1995), ontogenetic isotopic sampling was focused on the outer layer. However, this was either impossible (because it had flaked away before resin-encasement) or inadvisable (because it had a spongy appearance possibly reflecting chemical alteration) in specimens of *C. squamulosa ampla*, so material was taken from the m+1 layer (middle layer outside the pallial myostracum; Bieler et al., 2014). In *A. islandica* specimen 5 it was discovered retrospectively by examining the sampling path that some samples had included inner-layer material (Fig. 4B), and a few were largely or entirely from the inner layer. As the latter were in a sequence parallel, rather than transverse, to annual growth lines they did not form a time series and the data from them has consequently been discarded.

Sampling of shell cross-sections (*A. islandica*, *C. squamulosa ampla*) was conducted by a mixture of drilling and milling (Schöne et al., 2005a). The former technique (employing a vice-mounted hand drill) was used for annual increment 3 of *A. islandica* specimen BRS-AJ1-CC-D1R and for sampling of all other sectioned shells (employing a computer-controlled drill); sample spacing was about 1 mm. The latter technique (again employing a vice-mounted drill, but equipped with a cylindrical bit) was used for whole-increment sampling of annual increments 4–16 in BRS-AJ1-CC-D1R and for sub-sampling (9–17 steps per increment) of increments 17–25. Sampling of the external surface (*A. opercularis*, *L. borealis*, *P. maxima*) was by hand-held drill, used to cut shallow pits or grooves parallel to

commarginal striae (*A. opercularis*). In the case of *P. maxima* the thin primary layer was drilled away before sampling the secondary layer. Sample weights were 50–200 μg.

2.7.2. Spot and whole-shell sampling

Spot samples were taken by drilling the external surface (outer layer) using a computer-controlled drill. In most cases a single, randomly positioned sample was taken from a shell (e.g., Fig. 3A, E, F). Where more were extracted, these were taken from points representing different times in ontogeny (e.g., Fig. 3B). Sample weights were 50–200 μg.

Specimens for whole-shell sampling were less than 3 mm in size but in some cases constituted fragments of somewhat larger individuals (e.g., Fig. 3H). Specimens were crushed using a pestle and mortar. A 50–200 μg aliquot of the resultant powder was taken and the rest discarded.

2.8. Isotopic analysis

Measurement of oxygen and carbon isotope ratios (reported as $\delta^{18}O$ and $\delta^{13}C$; ‰) was carried out in laboratories at Cambridge, Keyworth, Mainz and Frankfurt (data spanning ontogenetic year 3 of *A. islandica* specimen BRS-CC-AJ1-D1R, previously reported in Johnson et al., 2009). Analysis in Cambridge, Mainz and Frankfurt involved a Thermo Finnigan MAT 253 continuous flow, isotope ratio mass spectrometer coupled to a Gasbench II. Powder samples were dissolved with concentrated phosphoric acid in helium-flushed borosilicate exetainers at 70 °C (Cambridge) or 72 °C (Mainz, Frankfurt). Analysis at Keyworth involved an Isoprime dual inlet mass spectrometer coupled to a Multiprep system. Powder samples were dissolved with concentrated phosphoric acid in borosilicate wheeton vials at 90 °C. All laboratories calibrated their $\delta^{18}O$ and $\delta^{13}C$ data against NBS-19 and their

own Carrara marble standard. Internal precision (1σ) was < 0.1‰ for $\delta^{18}O$ and $\delta^{13}C$. Isotope values were calculated against the Vienna Pee Dee Belemnite (VPDB) and Craig-corrected (McKinney et al., 1950).

2.9. Temperature calculation

To conform to previous work on modern, subfossil and Pliocene *A. opercularis* (Hickson et al. 1999, 2000; Johnson et al., 2000, 2009; Valentine et al. 2011), temperatures were derived from the $\delta^{18}O$ of calcite from this and other species using the calcite-water fractionation expression of O'Neil et al. (1969), as expanded about 16.9 °C by Shackleton (1974) into the following equation:

$$T\ (°C) = 16.9 - 4.38\ (\delta^{18}O_{calcite} - \delta^{18}O_{water}) + 0.1\ (\delta^{18}O_{calcite} - \delta^{18}O_{water})^2 \quad (1)$$

A linear regression fitted to the temperature and '1000 ln(alpha)' data of O'Neil et al. (1969) for values in the environmental range (temperatures ≤ 25 °C) has an intercept (temperature = 142.2 °C) with a 2σ-error of 9.3 °C. Although this is large, the $\delta^{18}O$ of modern *A. opercularis* is close to that predicted from an alternative formulation of equation (1), using measured values of temperature and water $\delta^{18}O$ for the area and time of shell formation (Hickson et al., 1999). Negative offsets of *c.* 0.5–1.0‰ (*c.* 2–4 °C) in winter are almost certainly due largely to 'missing' shell as a result of growth interruptions. Similar or smaller negative summer offsets may reflect a tendency for temperatures to be slightly overestimated using the O'Neil/Shackleton relationship. The more recent equation of Kim and O'Neil (1997), similarly based on synthetic calcite but giving temperatures 1–2 °C lower

(Bemis et al., 1998, table 1), may therefore be a little more accurate for *A. opercularis*, and by implication other calcitic species.

We subtracted 0.27‰ from our water $\delta^{18}O$ values (measured against SMOW) in order to adjust them to the VPDB scale used for shell carbonate (Gonfiantini et al., 1995). This adjustment was incorporated in a modified version of the aragonite equation of Grossman and Ku (1986), based on data from foraminifers and mollusks, for calculation of temperatures from aragonitic species:

$$T\ (°C) = 20.60 - 4.34\ (\delta^{18}O_{aragonite} - (\delta^{18}O_{water} - 0.27)) \quad (2)$$

A linear regression fitted to the temperature and 'shell $\delta^{18}O$ – water $\delta^{18}O$' data of Grossman and Ku (1986) has an intercept (temperature = 20.3 °C) with a 2σ-error of 1.2 °C.

We calculated temperatures using the four initial values for water $\delta^{18}O$ employed by Johnson et al. (2009): the most divergent global average estimates for the Pliocene from deep-sea foraminiferal data (–0.5‰, –0.2‰; Buchardt and Símonarson, 2003) and the most divergent site-specific estimates for the Coralline Crag from modelling (+0.1‰, +0.5‰; Johnson et al., 2009, p. 172). Equation (1) is non-linear and with the highest value for water $\delta^{18}O$ (+0.5‰) yields a temperature 3.8 °C higher than with the lowest value for water $\delta^{18}O$ (–0.5‰) for the highest shell (calcite) $\delta^{18}O$ measured (+2.69‰), and 4.5 °C higher for the lowest shell $\delta^{18}O$ measured (–0.69‰). Equation (2) is linear and with the highest value for water $\delta^{18}O$ yields a temperature 4.3 °C higher than with the lowest value for water $\delta^{18}O$ for any value of shell (aragonite) $\delta^{18}O$.

Note that $\delta^{18}O$ of shell aragonite was not corrected for different acid-fractionation factors of aragonite and calcite (for further explanation, see Füllenbach et al., 2015).

3. Results

3.1. Outcomes of preservation tests

In all 13 taxa investigated by SEM there was revealed excellent preservation of both calcite (foliated and fibrous) and aragonite (homogeneous, crossed lamellar, complex crossed lamellar, composite prisms) microstructures (e.g., Fig. 5), which were the same as those from related modern taxa (e.g., Williams, 1990; Bieler et al., 2014). *A. islandica* did not show changes observed in the experimental diagenesis of that species (Casella et al., 2017). Blocky, diagenetic calcite was rarely seen in any of the shells, or in microborings or brachiopod punctae (Fig. 5B). These observations confirm the findings of earlier SEM work on *A. opercularis* (Johnson et al., 2009).

One specimen of the aragonitic species *C. squamulosa ampla* (specimen 7) showed patches of dull orange cathodoluminescence (Fig. 6B, C) amongst more widespread blue luminescence, which reflects the original aragonite and was seen ubiquitously in the three other specimens of *C. squamulosa ampla* investigated by CL (e.g., 8; Fig. 6A) and in the two of *A. islandica*. The crossed-lamellar structure (developed only in aragonite) evident within the patches (Fig. 6C) and their gradational boundaries (contrary to what would be expected of areas containing diagenetic calcite crystals; J.A.D. Dickson, personal communication, 2017), make it doubtful that the patches mark alteration (see also section 3.2.2). Manganese (the cause of orange cathodoluminescence) is incorporated into the shell of aragonitic bivalves in varying amounts during growth (e.g., Zhao et al., 2017), and it is conceivable that the patches of orange luminescence seen in *C. squamulosa ampla* specimen 7 relate to times of particularly high uptake. Certainly, cathodoluminescence in bivalves is affected by environmental factors during life and must be interpreted with care (Barbin et al., 1991).

The mineralogy of *C. squamulosa ampla* specimen 7, as revealed by XRD, was 97% aragonite (± 1–2%), the same as in the other *C. squamulosa ampla* specimen (specimen 1; showing only blue luminescence) investigated by XRD. The investigated specimen of *S. arcuata* was *c.* 99% aragonite. These results indicate minimal alteration. All the XRD spectra are available as Supplementary Material B.

3.2. Ontogenetic isotope data

Where annual growth lines were identified (*A. islandica*, *C. squamulosa ampla*), isotope values have been plotted against ontogenetic year, with numbered year-markers corresponding to the positions of annual growth lines and representing the end of the year concerned (Figs. 7, 8). Where independent evidence of age was unavailable (*A. opercularis*, *P. maxima*, *L. borealis*), values have been plotted against linear distance from the origin of growth, measured along the axis of maximum growth (Figs. 9–11). The range, mean and standard deviation for summer $\delta^{18}O$ minima and winter $\delta^{18}O$ maxima in each specimen and taxon are shown diagrammatically in Fig. 12A. Range, mean and standard deviation for $\delta^{13}C$ values are given in Fig. 12B.

3.2.1. A. islandica

In *A. islandica* specimen BRS-AJ1-CC-D1R (Fig. 7A), those years (3, 17–25) sampled at high resolution show a well-defined annual cyclicity in $\delta^{18}O$, with minima nearly always a little after annual growth lines and maxima roughly half-way between. $\delta^{13}C$ parallels $\delta^{18}O$ in some years (r up to 0.89) but at other times (e.g., over the end of year 21 and start of year 22) is markedly out of phase ($r = –0.58$ for 15 samples between the $\delta^{18}O$ maxima for years 21 and 22). The low-resolution data for years 4–16 plot within the range of the high-resolution

data with the exception of $\delta^{13}C$ values for years 6 and 8, which slightly exceed the maximum in the high-resolution data.

A. islandica specimens 1, 2 and 5 (Fig. 7B–D), sampled at intermediate resolution, do not show such a well-defined cyclicity in $\delta^{18}O$; nevertheless, the number of peaks and troughs approximately corresponds to the number of years indicated by growth lines, at least for specimens 1 and 2. Given the 'noise' in the $\delta^{18}O$ profile from specimen 5 (possibly accountable to inclusion of some inner-layer material; see section 2.7.1), it was considered appropriate to recognise only one maximum and one minimum $\delta^{18}O$ value (both year 3). $\delta^{13}C$ shows some parallels with $\delta^{18}O$ in specimen 5 (r = 0.58 overall) but no real parallels in specimens 1 and 2.

In BRS-AJ1-CC-D1R the mean minimum and maximum $\delta^{18}O$ values are +1.76 ± 0.27‰ (± 1σ) and +2.52 ± 0.17‰, respectively (Fig. 12A). The mean (or singleton) minima and maxima for specimens 1, 2 and 5 range from +1.96 to +2.34‰ (mean +2.09 ± 0.17‰) and +2.63 to +2.94‰ (mean +2.78 ± 0.13‰), respectively. There is a strong positive correlation (r = 0.95) between mean individual minima and maxima. It is unlikely that the lower mean minimum and maximum of BRS-AJ1-CC-D1R compared to the other specimens is due to higher resolution sampling; this should yield a higher mean maximum through inclusion of shell material with the most positive $\delta^{18}O$.

Mean individual values for $\delta^{13}C$ span a range of 0.73‰ (Fig. 12B). The species mean is +2.91 ± 0.31‰.

3.2.2. C. squamulosa ampla

Although only sampled at intermediate resolution, all four specimens show a fairly well-defined cyclicity in $\delta^{18}O$, with maxima nearly always at annual growth lines (Fig. 8A-D). Mean individual values for summer $\delta^{18}O$ minima and winter $\delta^{18}O$ maxima range from +1.35

to +2.08 ‰ (mean +1.82 ± 0.28‰) and +2.04 to +2.42‰ (mean +2.28 ± 0.15‰), respectively (Fig. 12A). There is a strong positive correlation (r = 0.95) between mean individual minima and maxima. The taxon mean for summer minima is slightly lower than that from *A. islandica* specimens 1, 2 and 5 (likewise sampled at intermediate resolution) and the taxon mean for winter maxima is more markedly lower than that from *A. islandica* specimens 1, 2 and 5. The winter discrepancy may be accountable to the growth breaks represented by growth lines at the positions of maximum $\delta^{18}O$ (i.e., failure to deposit material with higher $\delta^{18}O$).

$\delta^{13}C$ shows weak parallels with $\delta^{18}O$ in specimen 8 (r = 0.39 overall) but no real parallels in specimens 1, 7 and 10. Mean individual values for $\delta^{13}C$ span a range of 0.71‰ (Fig. 12B). The taxon mean for $\delta^{13}C$ (+2.34 ± 0.28‰) is lower by 0.57‰ than that from *A. islandica*.

Both the $\delta^{18}O$ and $\delta^{13}C$ means from specimen 7 occupy a central position in the respective ranges for this taxon, suggesting that the shell is unaltered, despite some indications from cathodoluminescence to the contrary (section 3.1).

3.2.3. A. opercularis

Both specimens show one well-defined cycle in $\delta^{18}O$ incorporating a clear summer and winter inflection (Fig. 9A, B). It is possible to recognise a second (later) summer minimum in UD 53361 but 'noise' makes it difficult to define a second (earlier) winter maximum. Although not associated with an inflection it is reasonable to take the high value at the start of the profile from UD 53360 as a winter 'maximum' because it is substantially greater than the later winter maximum and clearly not representative of noise. The species means for summer minima (+0.44 ± 0.30‰) and winter maxima (+1.86 ± 0.02‰) are lower than the equivalents from *A. islandica* and *C. squamulosa ampla* (Fig. 12A), and also lower than the more strictly comparable (high resolution) values from *A. islandica* specimen BRS-AJ1-CC-D1R (section

3.2.1). A difference of 0.8‰ is to be expected because for a given temperature and water $\delta^{18}O$ the equilibrium calcite value is lower than the aragonite value by that amount (Kim et al., 2007). However, the discrepancy for mean summer minimum is 1.32‰ with *A. islandica* specimen BRS-AJ1-CC-D1R. This larger difference than expected may be accountable to rapid growth in *A. opercularis* over summer intervals and sampling at exceptionally high temporal resolution, resulting in inclusion of material with the most negative $\delta^{18}O$ (note the relatively broad summer sectors containing numerous sample points in Fig. 9A, B).

$\delta^{13}C$ shows some parallels with $\delta^{18}O$ in both UD 53360 and 53361 (r = 0.53 overall in each) and mean individual values for $\delta^{13}C$ are very similar (+0.39 ± 0.16‰ and +0.41 ± 0.37‰, respectively). The species mean (+0.40 ± 0.01‰; Fig. 12B) is lower than from *A. islandica* and *C. squamulosa ampla* by 2.51‰ and 1.94‰, respectively. This is largely accountable to mineralogical differences in that $\delta^{13}C$ in calcite is generally 1.4–2.0‰ lower than in co-precipitated aragonite (Krantz et al., 1987).

3.2.4. P. maxima

Specimen 1 shows three well-defined cycles in $\delta^{18}O$ (Fig. 10A). The mean values for summer $\delta^{18}O$ minima and winter $\delta^{18}O$ maxima are +0.25 ± 0.49‰ and +1.46 ± 0.22‰, respectively (Fig. 12A). Specimen 2 shows only an incomplete $\delta^{18}O$ cycle but it is possible to recognise a summer minimum and winter maximum. The species means for summer minima (+0.58 ± 0.33‰) and winter maxima (+1.90 ± 0.44‰) are close to those from *A. opercularis* (Fig. 12A) and similarly accountable to calcitic mineralogy and sampling at exceptionally high temporal resolution over summer intervals (note the relatively broad summer sectors containing numerous sample points in Fig. 10A).

$\delta^{13}C$ shows parallels with $\delta^{18}O$ in both specimen 1 (r = 0.83) and specimen 2 (r = 0.96) but mean individual values for $\delta^{13}C$ differ by 1.00‰ (Fig. 12B). The species mean (–0.34 ±

0.45‰) is substantially lower than that from the similarly calcitic *A. opercularis*, and probably too far below the equivalent values from the aragonitic taxa *A. islandica* and *C. squamulosa ampla* (differences of 3.25‰ and 2.68‰, respectively) to be accountable entirely to mineralogy.

3.2.5. L. borealis

The $\delta^{18}O$ profile from *L. borealis* specimen 3 (Fig. 11A) may depict two annual cycles, but the amount of variation is small and might reflect 'noise'. In view of the likely growth rate (see section 3.2), the two minima and maxima have been taken to represent summers and winters. The 'summer' mean (+1.79 ± 0.07‰) is within the ranges of summer means from specimens of the similarly aragonitic *A. islandica* and *C. squamulosa ampla* sampled at intermediate resolution (Fig. 12A). The 'winter' mean (+2.16 ± 0.00‰) is likewise within the winter range from *C. squamulosa ampla* but substantially below the lowest mean from *A. islandica.*

$\delta^{13}C$ shows no parallels with $\delta^{18}O$. The mean value for *L. borealis* (–0.01 ± 0.45‰) is far below the ranges of individual means for the similarly aragonitic *A. islandica* and *C. squamulosa ampla* (Fig. 12B). This may reflect reducing conditions in the sediment at the sites occupied by this chemosymbiotic species; these would have caused porewater $\delta^{13}C$ to be particularly low (Presley and Kaplan, 1970; Claypool and Threlkeld, 1983).

3.3. Microgrowth-increment data

The microgrowth increment profiles from *A. opercularis* specimens UD 53360 and 53361 quite closely parallel the respective profiles for $\delta^{18}O$ and thus show an approximately annual

fluctuation (Fig. 9A, B). The amplitude of this variation is fairly high in the former: over 0.3 mm between maximum and minimum of the smoothed profile.

3.4. Temperatures from ontogenetic $\delta^{18}O$ data

The four values for water $\delta^{18}O$ given and explained in section 2.9 have been used with equations (1) and (2), as appropriate, to generate temperature profiles (Figs. 7E–H; 8E–H; 9C, D; 10C, D; 11B) from the shell $\delta^{18}O$ data. As can be seen (e.g., Figs. 7F, G; 9D; 10D), the lowest value for water $\delta^{18}O$ (–0.5‰; a global average estimate) yields a number of temperatures under 5 °C, which is at odds with benthic ostracod (Wood et al., 1993) and bryozoan (Taylor and Taylor, 2012) assemblage evidence that winter temperatures in the Coralline Crag sea were at least as high as in the modern North Sea adjacent to the collection locations of the specimens (typical winter minimum, 6–7 °C). For this reason, temperatures generated using –0.5‰ for the $\delta^{18}O$ of ambient water are not considered credible (the same applies to temperatures down to 3.6 °C from *A. islandica* specimens 1, 2 and 5, calculated using a water $\delta^{18}O$ value of –0.35‰; see section 1). Amongst the other water $\delta^{18}O$ values, we favour the two highest values because these were generated by modelling for the specific area concerned, and of these we prefer +0.1‰ because it is intermediate between the other modelled local estimate (+0.5‰) and an alternative global estimate (–0.2‰). Temperature profiles calculated using a water value of +0.1‰ are indicated by use of a thicker (orange) line in Figures 7–11 to signify our preference. Temperatures discussed in the following are from these data, except where indicated otherwise. The range, mean and standard deviation for summer temperature maxima and winter temperature minima in each specimen and taxon, based on a water $\delta^{18}O$ value of +0.1‰, are shown diagrammatically in Fig. 13.

3.4.1. A. islandica

The temperature profiles from all four specimens (Fig. 7E–H) show large sectors below 10 °C (the upper boundary for winter temperature in a cool temperate marine climate), and the individual means for winter temperature minima (Fig. 13) are well below this figure. None of the specimens show temperatures above 20 °C (the upper boundary for summer temperature in a cool temperate marine climate) and the individual means for summer temperature maxima are far below this figure (below 15 °C). The overall mean temperature (mean of all the temperatures from the four profiles combined) is 10.2 ± 1.5 °C (± 1σ). The positive correlation noted between individual mean $\delta^{18}O$ minima and maxima (section 3.2.1) indicates that individuals lived under differing overall temperature regimes (slightly warmer/cooler). For years sampled at high resolution in BRS-AJ1-CC-D1R the mean temperature (average of all data) is 10.4 ± 1.3 °C, close to the figure of 11.1 ± 0.8 °C for the mean of temperatures derived from low-resolution (annual) sampling of other years.

Using a water $\delta^{18}O$ value of +0.5‰ still yields temperatures below 10 °C from all shells except specimen 5, and no shell yields a temperature above 20 °C.

The temperatures obtained from Coralline Crag *A. islandica* are very largely consistent with the cool temperate occurrence of modern representatives (section 2.1).

3.4.2. C. squamulosa ampla

The temperature profiles from all four specimens show sectors below 10 °C (Fig. 8E–H), but the proportions below are smaller than in *A. islandica*. Two of the individual means for winter temperature minima (Fig. 13) are below 10 °C, but the amounts below are smaller than in *A. islandica* sampled at the same (intermediate) resolution. None of the specimens show temperatures above 20 °C and the individual means for summer temperature maxima are far

below this figure (below 15 °C). The overall mean temperature is 11.0 ± 1.4 °C. The positive correlation noted between individual mean $\delta^{18}O$ minima and maxima (section 3.2.2) indicates that individuals lived under differing overall temperature regimes (slightly warmer/cooler).

Using a water $\delta^{18}O$ value of +0.5‰, only specimen 1 yields a temperature below 10 °C but none of the shells yields a temperature above 20 °C.

The divergence in winter temperature data from those supplied by *A. islandica* may be accountable to winter growth breaks signified by growth lines (section 3.2.2), i.e., the *C. squamulosa ampla* specimens may have experienced (but not recorded) much the same winter minimum temperatures as the *A. islandica* specimens. Even if the winter minimum temperatures experienced by the *C. squamulosa ampla* specimens were slightly higher, at least some of those calculated with a water $\delta^{18}O$ of +0.1‰ are in the cool temperate range. The occurrence of winter rather than summer growth breaks is consistent with a cool temperate interpretation (Jones and Quitmyer, 1996). This contrasts with the warm temperate marine climate associated with the close modern relative *C. antiquatus* (Fig. 3D; section 2.1).

3.4.3. A. opercularis

The temperature profiles from both specimens (Fig. 9C, D) show sectors below 10 °C, and the individual mean/singleton values for winter temperature minima (Fig. 13) are well below this figure and similar to values from *A. islandica* sampled at both high and intermediate resolution. Neither of the specimens shows temperatures above 20 °C and the individual mean/singleton values for summer temperature maxima are far below this figure. The overall mean temperature is 11.3 ± 2.2 °C.

Johnson et al. (2009, table 3) provided figures for the extreme minimum and maximum temperatures from $\delta^{18}O$ profiles of eight other *A. opercularis* shells from the Ramsholt Member of the Coralline Crag Formation. For a water $\delta^{18}O$ of +0.1‰ the respective means

are 7.7 ± 0.9 °C and 14.4 ± 1.4 °C. These figures are indistinguishable from the equivalent means of 8.1 ± 0.3 °C and 14.4 ± 1.1 °C from the two ontogenetically sampled Ramsholt Member shells of the present study.

Using a water $\delta^{18}O$ value of +0.5‰ still yields temperatures below 10 °C from the two shells analysed in the present study, and neither yields a temperature above 20 °C.

The temperatures obtained from Coralline Crag *A. opercularis* are in the cool temperate range and entirely consistent with the cool (and warm) temperate occurrence of modern representatives (section 2.1).

3.4.4. P. maxima

The temperature profiles from both specimens (Fig. 10C, D) show sectors below 10 °C. The individual mean for winter temperature minima from specimen 1 is 10 ± 0.9°C and the singleton value from specimen 2 is 6.5 °C, the former value being a little higher than the mean minima from other specimens sampled at high resolution (*A. islandica* BRS-AJ1-CC-D1R and both specimens of *A. opercularis*; Fig. 13). Neither of the specimens shows temperatures above 20 °C and the individual mean/singleton values for summer temperature maxima are far below this figure. The overall mean temperature is 12.4 ± 2.8 °C.

Using a water $\delta^{18}O$ value of +0.5‰ still yields temperatures below 10 °C from specimen 2 and neither specimen yields a temperature above 20 °C.

The temperatures obtained from *P. maxima* are lower than expected from the occurrence of fossil relatives.

3.4.5. L. borealis

The temperature profile from the specimen (Fig. 11B) does not show any sectors below 10 °C. The individual means for winter temperature minima and summer temperature maxima Fig. 13) are 10.5 °C and 12.1 °C, respectively. Both are within the ranges of individual means from *C. squamulosa ampla* (similarly sampled at intermediate resolution). The overall mean temperature is 11.4 ± 0.7 °C.

Using a water $\delta^{18}O$ value of +0.5‰ does not yield any temperatures above 20 °C.

The mean for winter temperature minima is slightly above the cool temperate range but this could easily reflect insufficiently close sampling to detect cooler temperatures. The temperatures obtained are entirely consistent with the warm and cool temperate occurrence of modern *L. borealis* (section 2.1).

3.5. Temperatures from spot and whole-shell $\delta^{18}O$ data

Since, unlike the ontogenetic data, the spot and whole-shell $\delta^{18}O$ data cannot be meaningfully and usefully compared with ontogenetic $\delta^{13}C$ and microgrowth-increment data, there is no merit in presenting them in their own right. Instead, they are given translated into temperatures by the methods employed for ontogenetic data (see section 2.9), using the same four water $\delta^{18}O$ values. Figure 14 shows the 81 sets of four temperatures obtained, arranged in order of increasing temperature to the right within taxa, with the number of specimens indicated in each case. Included are markers of mean spot/whole-shell temperature for each taxon based on a water $\delta^{18}O$ of +0.1‰, markers of overall mean, mean summer maximum and mean winter minimum temperature from ontogenetic data (using a water $\delta^{18}O$ value of +0.1‰), and markers of average summer maximum and average winter minimum temperature (surface and seafloor) in the well-mixed southern North Sea at present.

Temperatures quoted in the following subsections are based on a water $\delta^{18}O$ of +0.1‰, except where stated otherwise.

3.5.1. Temperatures from spot data

For taxa that were also investigated ontogenetically (*A. opercularis*, *C. squamulosa ampla*, *L. borealis*, *A. islandica*, *P. maxima*), 'spot' temperatures fall between the relevant mean summer maximum and mean winter minimum from ontogenetic data in 14 of the 23 cases. These instances provide confirmation that the ontogenetically analysed specimens of the taxa concerned (all but *A. islandica*) are representative of those taxa in terms of the temperatures at which they lived. Of the remaining nine spot temperatures, one from *A. opercularis* is above the mean summer maximum from ontogenetic data, but so far above this value (which is corroborated by previously published results; see section 3.4.3), and also the other nine spot temperatures from *A. opercularis*, that it must be considered a suspect datum, possibly a product of contamination in sampling. The eight spot temperatures below the relevant mean winter minimum are constituted by single cases in each of *A. opercularis*, *C. squamulosa ampla* and *L. borealis*, and all of the five cases in *A. islandica*. Four of the *A. islandica* instances are below the lowest mean individual winter minimum (7.1 °C; specimen 1) and two (5.4, 6.0 °C) are below the lowest single winter minimum (6.4 °C; specimen 1) recorded amongst the ontogenetically analysed specimens. This suggests that the latter may be unrepresentative—i.e., they lived under slightly warmer conditions than was typical for Coralline Crag *A. islandica*. The same conclusion would apply for comparisons of temperatures derived using other water $\delta^{18}O$ values.

The taxon means for spot temperatures from the other eight species investigated in this way range from 5.8 °C to 12.5 °C, with a grand mean (mean of means) of 9.7 ± 2.4 °C. These figures compare closely with the equivalents (6.5–11.9 °C; 9.6 ± 1.8 °C) from the five species

that were also investigated ontogenetically, suggesting that these are representative of the Coralline Crag biota as a whole in terms of the range of temperatures at which taxa lived.

Of the eight species investigated through spot sampling alone, only the 'warm' species *T. multistriata* yields temperatures at odds with the relevant 'warm', 'cool' or 'eurythermal' designation. Of the five values from *T. multistriata*, one from each of the two specimens investigated (5.5, 6.1 °C) is well below the lower threshold of 10 °C for the warm temperate marine climate with which *T. multistriata* is now associated (section 2.1), and indeed below the average winter minimum temperature in the southern North Sea at present (Fig. 14). The equivalent temperatures calculated using a water $\delta^{18}O$ value of +0.5‰ (respectively, 7.0, 7.6 °C) are still substantially below the 10 °C threshold.

3.5.2. Temperatures from whole-shell data

The temperature ranges from whole-shell sampling of *C. corbis*, *R. conuloidea* and *R. buccinea* are, respectively, 8.8–12.7 °C, 7.2–10.1 °C and 10.5–13.4 °C. The combined range (7.2–13.4 °C) extends to values a little above the grand mean (mean of taxon means) for summer maximum temperature from ontogenetic sampling (12.6 ± 1.2 °C) and extends rather more below the grand mean for winter minimum temperature from ontogenetic sampling (9.1 ± 1.0 °C). However, the range of temperatures from whole-shell sampling does not exceed the upper limit of taxon means for summer maximum temperature from ontogenetic sampling (highest value 14.3 °C, from *A. opercularis*), although it extends below the lower limit of taxon means for winter minimum temperature from ontogenetic sampling (lowest value 8.1 °C, from *A. islandica*).

The mean temperatures from whole-shell sampling of *C. corbis*, *R. conuloidea* and *R. buccinea* are, respectively, 10.5 ± 1.4 °C, 8.6 ± 1.1 °C and 11.6 ± 0.9 °C. These mean temperatures do not exceed the upper limit of taxon means (using all data points) from

ontogenetic sampling (highest value 12.4 °C, from *P. maxima*) but extend below the lower limit (10.2 °C, from *A. islandica*).

The whole-shell data in part support the conclusion from spot data that the ontogenetically sampled taxa are representative of the Coralline Crag biota as a whole, but conflicting evidence is provided by individual and taxon mean temperatures from whole-shell sampling that are below the taxon means for winter minimum (and overall mean) temperature from ontogenetic sampling. This could partly reflect the nature of the data (the taxon means for winter minimum temperature are averages of averages and hence conservative estimates) or be a consequence of growth only during winter in the taxa used for whole-shell sampling (the individuals sampled were small enough to have lived only a few months—complete shells < 5 mm; Fig. 3H)

Of the three species investigated through whole-shell sampling, *R. conuloidea* and *R. buccinea* give temperatures consistent with their designation as 'cool' and 'warm' species, respectively. However, *C. corbis* gives temperatures at odds with its designation as a 'warm' species. Of the nine temperatures from *C. corbis*, four (8.8, 9.1, 9.2, 9.6 °C) are below the lower threshold of 10 °C for the warm temperate marine climate with which this species is now associated (section 2.1). The equivalent temperatures calculated using a water $\delta^{18}O$ value of +0.5‰ (10.5, 10.8, 11.0, 11.3 °C, respectively) are, however, above the 10 °C threshold.

4. Discussion

4.1. Relative temperatures

Although resolution was not uniform amongst the five taxa sampled ontogenetically, this is unlikely to have significantly biased overall taxon mean temperatures, making comparisons involving this parameter valid. Using, as previously, a common value for water $\delta^{18}O$ (+0.1‰), the overall taxon mean for *A. islandica* (10.2 ± 1.5 °C) is lower than for *C. squamulosa ampla* (11.0 ± 1.4 °C) and *P. maxima* (12.4 ± 2.8 °C). This is in accordance with the notion of the first as a 'cool' taxon and the last two as 'warm' taxa, and with the idea of fluctuating marine climate during deposition of the Coralline Crag. The means of spot data show a similar pattern (i.e., lower for *A. islandica* than for *C. squamulosa ampla* and *P. maxima*; Fig. 14), as do the taxon means for seasonal temperatures (Figs. 13, 14). However, in the latter case sampling resolution is a potential biasing factor so comparisons must be made more carefully. The (restricted) taxon means for winter minimum and summer maximum temperature from the three specimens of *A. islandica* sampled at intermediate resolution (7.8 ± 0.5 °C and 10.8 ± 0.8 °C, respectively) are lower than the equivalent means from *C. squamulosa ampla* (9.9 ± 0.6 °C and 12.0 ± 1.2 °C, respectively), likewise sampled at intermediate resolution. Similarly, the individual mean for summer maximum temperature from the *A. islandica* specimen sampled at high resolution (12.2 ± 1.2 °C) is lower than the taxon mean from *P. maxima* (13.7 ± 1.4 °C), likewise sampled at high resolution. While the individual mean for winter minimum temperature from the *A. islandica* specimen (8.9 ± 0.7 °C) is higher than the taxon mean from *P. maxima* (8.3 ± 1.8 °C), it is lower than the individual mean from *P. maxima* specimen 1 (10.0 ± 0.9 °C). Thus the pattern in the seasonal temperature data largely matches, and therefore to the same extent corroborates, the pattern seen within the data for overall taxon mean temperature (and amongst spot-temperature means).

Irrespective of their statistical significance, there are only small differences between the values from 'cool' and 'warm' species for overall taxon mean temperature from ontogenetic data. Unsurprisingly, the range of variation (2.2 °C) is not expanded by inclusion of values from the 'eurythermal' species *A. opercularis* (11.3 ± 2.2 °C) and *L. borealis* (11.4 ± 0.7 °C). At most, therefore, we can only infer small fluctuations in marine climate from these data. As we have noted, within both *A. islandica* and *C. squamulosa ampla* there is covariation between individual mean $\delta^{18}O$ minima and maxima, indicating that individuals of each of these taxa lived under slightly different overall temperature regimes. All species can, of course, tolerate some variation in mean conditions so such individual differences are entirely to be expected. We can use the most extreme individual data to gain a broader picture of temperature variation during Coralline Crag deposition. The lowest mean temperature from an *A. islandica* individual (average of all data) is from specimen 1 (8.3 ± 1.0 °C) and the highest from *C. squamulosa ampla* from specimen 8 (12.4 ± 1.4 °C). However, the value from the latter is exceeded by that from *P. maxima* specimen 1 (13.3 ± 2.3 °C). We might therefore infer that over intervals similar to individual lifespans average annual seafloor temperature was sometimes as much as 5 °C higher than over other such intervals during Coralline Crag deposition. Since we do not know the precise stratigraphic horizon of specimens we can say little about the separation in time of these inferred warmer and cooler phases. It might have been only slightly more than the lifespan of individuals or approaching the total time taken for deposition of the Coralline Crag. This period, as already noted, was probably long enough to include glacial and interglacial stages, and over a comparable timespan water-temperature changes at shallow–intermediate depths in the order of 5 °C have been documented during the Pliocene from mid-latitude sites in the North Atlantic (De Schepper et al., 2013; Bachem et al., 2016), while similar changes in continental air

temperature have been determined from the Netherlands (Dearing Crampton-Flood et al., 2018). It is therefore not unreasonable to explain the variation in individual mean temperatures from ontogenetically analysed specimens in terms of fluctuation in marine climate. The range in these data (8.3–13.3 °C) spans most of the equivalent spot and whole-shell temperatures (Fig. 14), and at least some of those temperatures outside it can be interpreted as representing seasonal extremes (or possibly sample contamination; see section 3.5.1). However, the preponderance of values below the lower bound, including some from whole-shell samples (*R. conuloidea*), suggests that the range of variation in annual average temperature extended to values somewhat lower than indicated by the ontogenetically analysed specimens, although probably not to values so low as to be beyond interpretation in terms of changes in marine climate between interglacial and glacial stages.

To this point we have focussed on the differences in temperature indicated by species, and individuals within species. However, it is important to recognise and explain similarities. For instance, while above we have identified ontogenetically analysed specimens of *A. islandica* and *C. squamulosa ampla* giving mean temperatures which differ substantially (by 4.1 °C), all three of the other ontogenetically analysed specimens of *C. squamulosa ampla* give mean temperatures (1: 10.3 ± 0.9 °C; 7: 10.4 ± 1.0 °C; 10: 10.7 ± 0.9 °C) which are indistinguishable from the mean temperature (10.4 ± 1.3 °C) given by *A. islandica* BRS-AJ1-CC-D1R. As noted previously (section 3.4.2), the association of growth lines/breaks with $\delta^{18}O$ maxima in *C. squamulosa ampla* suggests that individuals experienced winter temperatures lower than those recorded isotopically. The mean temperatures experienced may therefore likewise have been lower than those determined from the isotopic data and thus similar to the taxon mean for *A. islandica.* This would be contrary to the indication of temperature tolerance supplied by the restriction of the close modern relative *C. antiquatus* to the warm temperate setting of the Mediterranean, where *A. islandica* is absent. However, it is

entirely consistent with the observation of Long and Zalasiewicz (2011, p. 59), which we can confirm from our own fieldwork, that examples of *C. squamulosa ampla* and *A. islandica* occur abundantly alongside each other at certain horizons in the Coralline Crag.

The spot and whole-shell data provide evidence that other Coralline Crag taxa were living at temperatures different from modern representatives or close relatives. We have already noted that temperatures calculated with a water $\delta^{18}O$ of +0.1‰ from *T. multistriata* and *C. corbis* are in some cases below the lower limit for the warm temperate marine climate with which modern representatives of these species are associated (see, respectively, sections 3.5.1, 3.5.2). Continuing for the present with consideration of relative temperatures, we find that amongst the 11 taxa investigated only through spot and whole-shell sampling the mean of taxon means (grand mean) from the three 'warm' taxa (*T. multistriata, C. corbis, R. buccinea*) is, as expected, higher (10.6 ± 0.7 °C) than that (9.2 ± 1.8 °C) from the five 'cool' taxa (*G. obovata, A. gracilis, A. omalii, M. truncata, R. conuloidea*), However, the mean from *G. obovata* (11.9 ± 2.8 °C) is higher than the grand mean from warm taxa, and remains higher (10.7 ± 0.9 °C) even if a suspiciously high temperature value (17.8 °C; see Fig. 14) is excluded. Therefore, this appears to be another case where the temperature tolerance of a close modern relative (*G. glycymeris*) provides an inaccurate indication of the temperature at which a Coralline Crag species lived. However, it is possible that the equation of Grossman and Ku (1986) provides an overestimate of temperature from *G. obovata* (Royer et al., 2013).

4.2. Absolute temperatures

In the previous subsection we discussed whether temperatures calculated using a water $\delta^{18}O$ value of +0.1‰ conform with expectation in a relative sense—e.g., whether 'warm' taxa give higher temperatures than 'cool'. We can investigate the values themselves by checking

whether those from Coralline Crag *A. islandica* are as expected from the detailed information available on modern representatives of the species, specifically the fact that in the North Sea *A. islandica* is limited to areas where seafloor temperature does not exceed 16 °C (Witbaard and Bergman, 2003). Of the 22 summer temperatures recorded from Coralline Crag *A. islandica* the highest (from ontogenetic year 22 of BRS-AJ1-CC-D1R, which the individual lived two years beyond) is 15.1 °C. The equivalent temperature calculated using a water $\delta^{18}O$ value of +0.5‰ is 16.8 °C—i.e., above what appears to be tolerable by *A. islandica*. This strongly suggests that the water $\delta^{18}O$ value of +0.1‰ identified at the outset as the most reasonable is indeed a good approximation for Coralline Crag seawater. We can therefore regard all temperatures calculated using this value as 'correct', subject to the accuracy of the transfer functions used. As indicated in section 2.9, the errors on these are 1-2 °C for the temperature range of interest, with a tendency for the calcite function to overestimate temperature. The temperatures well below 10 °C recorded from numerous examples of the calcitic species *A. opercularis* (see section 3.4.3), together with specimens of *P. maxima*, *P. tigerinum* and *T. multistriata* (Figs. 13, 14), therefore seem entirely plausible, and a difference in temperature tolerance between modern and Coralline Crag examples of *T. multistriata* can hardly be denied. It remains possible that the relatively small 'discrepancies' in the temperature data from the aragonitic taxa *C. squamulosa ampla*, *C. corbis* and *G. obovata* are a reflection of error in the transfer function. One other firm and important point can, however, be made. This relates to the temperature supposedly indicated by the Coralline Crag bryozoan *Metrarabdotos moniliferum* on the basis of the restriction of modern congeners to areas where seafloor temperature never falls below 16 °C (Cheetham, 1967; Taylor and Taylor, 2012). All 16 of the taxa investigated isotopically give temperatures below this for a water $\delta^{18}O$ value of not only +0.1‰ but also +0.5‰ (Figs. 13, 14). To achieve a temperature of 16 °C from the high values of shell $\delta^{18}O$ recorded by many species

(e.g., values above +1.75‰ from the calcite of all 10 Ramsholt-Member *A. opercularis* specimens ontogenetically sampled to date) would require a water value in excess of +2‰. This is implausible given that global average water $\delta^{18}O$ is probably higher now than in the Pliocene (due to larger ice volume), yet even in the strongly evaporated setting of the Mediterranean Sea maximum water $\delta^{18}O$ is only +1.68‰ (Pierre, 1999). *M. monoliferum* occurs throughout the Coralline Crag (Taylor and Taylor, 2012) and it is inconceivable that it did not co-exist with any of the isotopically analysed species, some of which (e.g., *A. opercularis*) are similarly ubiquitous. It therefore seems clear that the tropical/subtropical present-day occurrence of *Metrarabdotos* is a false guide to the temperature tolerance of Pliocene *M. monoliferum*, perhaps reflecting a cold-induced contraction of range in the Pleistocene from which the genus has not yet recovered (cf. Taylor and Taylor, 2012).

4.3. Sea-surface temperatures

In the previous subsection we noted that all the investigated taxa provide isotopic temperatures below 16 °C with a water $\delta^{18}O$ value of +0.1‰. It is equally important to note that on the same basis very few provide temperatures above 16 °C, and amongst those that do, the values attained are never more than 20 °C. Amongst the 13 ontogenetically sampled specimens only *P. maxima* 1 provides temperatures (maximum 17.6 °C) above 16 °C, while amongst the 70 specimens investigated through spot and whole-shell samples just one of *A. opercularis* and one of *G. obovata* provide similar values (respectively, 19.2 and 17.8 °C; Fig. 14). The *G. obovata* datum is as aberrant as the *A. opercularis* one (see section 3.5.1), and so may likewise reflect contamination.

Of the eight Ramsholt-Member *A. opercularis* ontogenetically sampled by Johnson et al. (2009), one provided a temperature (16.2 °C) fractionally above 16 °C. On the basis of the

microgrowth-increment patterns from these *A. opercularis* specimens, together with biotic and sedimentological evidence, Johnson et al. (2009) concluded that the Ramsholt-Member sea was fairly deep (*c.* 50 m) and incompletely mixed in summer (i.e., thermally stratified). This interpretation would account for the modest summer seafloor temperatures in comparison to the surface temperatures of more than 20 °C indicated by pelagic dinoflagellate assemblages (Head, 1997, 1998). The *A. opercularis* specimens used in the present study show an approximately annual pattern of increment-size variation. similar to the specimens investigated previously, with the range of variation being over 0.3 mm in one (see section 3.3). Comparable ranges were recorded by Johnson et al. (2009, table 2) in three of five modern specimens from a 50 m-deep, seasonally stratified setting in the Gulf of Tunis (Mediterranean Sea) but in none of 14 specimens from well-mixed settings, as judged by being less than 25 m deep and/or meso- to macrotidal (hence subject to significant tidal currents). As well as the microgrowth-increment evidence of stratification from the present *A. opercularis* specimens, these and ontogenetically analysed specimens of *A. islandica* and *P. maxima* provide supporting evidence in the form of parallel variation of $\delta^{13}C$ with $\delta^{18}O$ (see sections 3.2.1, 3.2.3–4). This can be interpreted as a consequence of high seafloor respiration in summer, leading to release of isotopically light carbon for incorporation into shell carbonate alongside isotopically light oxygen, followed by autumn mixing down of surface waters containing isotopically heavy dissolved inorganic carbon (as a consequence of summer phytoplankton production in the surface layer) for incorporation into shell carbonate alongside isotopically heavy oxygen (e.g., Arthur et al., 1983; Krantz, 1990; Johnson et al., 2017). The critical element in this scenario is the separation of surface from deep waters in summer (i.e., enough warming to reduce density but insufficient agitation to cause mixing) such that a seafloor-surface gradient develops in the $\delta^{13}C$ of dissolved inorganic carbon. Johnson et al. (2009) considered it likely that the summer surface temperature of the

Ramsholt-Member sea was about 9 °C higher than seafloor temperature, and thus well into the warm temperate range. However, this view was based on a misreading of temperature data from the modern seasonally stratified setting of the Gulf of Tunis. While summer (August) temperature at 50 m (comparable to the depth of the Ramsholt Member sea) is indeed 9 °C below surface temperature in this area (17 °C, compared to 26 °C at the surface), autumn overturn of the water column results in seafloor temperatures of 21 °C in October/November (NOAA, 1994). Thus a more reasonable 'stratification factor' to add to maximum isotopic temperatures (9.7–15.5 °C for mean individual/singleton maxima from ontogenetically sampled specimens; Fig. 13) from the Ramsholt Member would be 5 °C. Even making an allowance of 2 °C for a possible underestimate of seafloor temperatures from aragonitic species, this only yields temperatures as high as 20 °C from three of the 13 ontogenetically sampled specimens, and two of the five sampled at high resolution. Hence, while summer maximum surface temperature was probably often 1–2 °C higher than at present (i.e., 17–19 °C rather than 16–17 °C), it was only sometimes in the warm temperate range. This deduction is supported by two other pieces of evidence. Firstly, as noted in section 3.2.1, around the end of ontogenetic year 21 and start of year 22 in *A. islandica* BRS-AJ1-CC-D1R the in-phase pattern of variation in $\delta^{13}C$ and $\delta^{18}O$ switches briefly to an antiphase pattern. This can be interpreted as a consequence of exceptional storminess, leading to mixing down of warm, high-$\delta^{13}C$ surface waters earlier than the normal, cooling-induced overturn in autumn. While the summer temperature in year 22 (15.1 °C) is higher than in any other, as would be expected with (atypical) summer circulation of surface waters to the seafloor, it is well short of 20 °C. Secondly, the single specimen of *A. opercularis* investigated by Johnson et al. (2009) from the current-swept, probably well-mixed setting of

the Sudbourne Member, yielded, as expected, a higher summer temperature than Ramsholt-Member forms (18.3 °C; using a water $\delta^{18}O$ value of +0.1‰), but again below 20 °C.

It is possible that the depth of the Ramsholt-Member sea insulated the seafloor somewhat from the effects of winter atmospheric cooling, as on the US Middle Atlantic shelf, where winter temperature is 2 °C higher at 30 m than at the surface (Winkelstern et al., 2013). The best estimates of winter minimum seafloor temperature, based on high-resolution sampling of *A.islandica* specimen BRS-AJ1-CC-D1R, *A. opercularis* and *P. maxima*, are 8–9 °C (Fig. 13). Taking a 2 °C insulating effect into account yields from these estimates a winter surface temperature of 6–7 °C, the same as in the southern North Sea at present (Fig. 14).

4.4. Early Pliocene climate and oceanography in the North Atlantic region

The isotopic evidence of cool early Pliocene conditions provided by the Ramsholt Member is matched by isotopic evidence from the basal part of the Sunken Meadow Member (Yorktown Formation) on the western side of the North Atlantic (Fig. 1; Johnson et al., 2017). While conditions were warmer during deposition of the upper part of the Sunken Meadow Member, they were not as warm as existed during deposition of higher members of the Yorktown Formation, much later in the Pliocene, as a consequence of a global rise in temperature (Johnson et al., 2017). The cool early Pliocene conditions evidenced on the eastern and western sides of the North Atlantic have also been revealed isotopically in Iceland (Gladenkov and Pokrovskiy, 1980; Buchardt and Símonarson, 2003), the cool temperatures deriving from the *Serripes* Zone. This has recently been dated by Verhoeven et al. (2011) to the mid-Zanclean (*c*. 4.0–4.5 Ma), overlapping the time of deposition of both the Ramsholt Member and Sunken Meadow Member. It is possible that the cool conditions represented in the three North Atlantic locations relate to a globally recognisable glacial

event at *c.* 4 Ma, whose cause is unclear (De Schepper et al., 2014). On the basis of a low mean $\delta^{13}C$ from Coralline Crag *A. opercularis* shells (+0.37‰) compared to pre-industrial Holocene *A. opercularis* shells (+0.79‰), Johnson et al. (2009) inferred relatively high atmospheric CO_2. The mean $\delta^{13}C$ from the further Coralline Crag *A. opercularis* shells analysed in this investigation (+0.43 ± 0.29‰; combined results from ontogenetic and spot sampling) corroborates the earlier result. If the interpretation in terms of atmospheric CO_2 is correct, one must look to other potential controls for the cool temperatures in the North Atlantic, and globally. Southward-flowing cool currents were influential in the western North Atlantic (Johnson et al., 2017). Large-scale cross-stratification, dipping to the south-west, is evidence of a strong, broadly southward flow during deposition of the Sudbourne Member of the Coralline Crag Formation. However, this undoubtedly reflects the dominant flow of tidal currents (Balson, 1999), and the southward direction of this was probably local, like the dominant southward flow on the western side of the southern North Sea at present (Wright et al., 1999, fig. 8.3a). Those depositional sedimentary structures not destroyed by bioturbation in the Ramsholt Member are of a smaller scale than in the Sudbourne Member. Given the mud content of the sediment, they are probably also a reflection of local (weaker) tidal currents. A remaining explanation for the temperatures measured or inferred from this unit is that they reflect global (atmospheric) warmth and withdrawal of oceanic heat supply by the Gulf Stream/North Atlantic Drift (Johnson et al., 2009). In that oceanic heat supply raises winter sea-surface temperature around Britain but has little influence on summer temperature, its withdrawal in the context of global warmth might be expected to yield winter temperatures much like those at present in the area of the southern North Sea and summer surface temperatures somewhat higher, as deduced herein for the early Pliocene of East Anglia.

5. Conclusions and further work

Our isotopic data in part confirm the 'mixed' temperature signal of the Coralline Crag (Williams et al., 2009), which we see as representing fluctuations in marine climate, possibly caused by changes in oceanic heat supply. However, marine climate appears to have been usually in the cool temperate range and never subtropical/tropical, as suggested by the bryozoan assemblage. The misleading indication given by this, and to a smaller extent by other elements of the biota (e.g., ostracods), is a caution to paleoenvironmental interpretation solely by analogy with modern forms: 'ecological uniformitarianism' is essentially a sound methodology, but not infallible.

We have suggested one explanation (slow 'rebound' from the effects of severe Pleistocene cooling) for the current subtropical/tropical distribution of the bryozoan *Metrarabdotos.* Change in temperature tolerance/preference over time is another potential explanation for the presence of this and other 'warm' taxa in the cool seafloor setting of the Coralline Crag. A further possibility is that their occurrence there was enabled by the existence of relatively warm surface waters—i.e., conditions during the pelagic larval stage, rather than in the benthic adult stage, are the real determinant of distribution. This idea, whose germ is in the thoughts of Raffi et al. (1985) and Long and Zalasiewicz (2011), is open to experimental test on modern forms. The complex behavioural responses of *A. islandica* larvae to changes in temperature and pressure certainly indicate great sensitivity to environmental conditions at this developmental stage (Mann and Wolf, 1983).

As well as the suggested experimental work it would be worth expanding $\delta^{18}O$-based investigations of Coralline Crag temperature to include other benthic taxa, in particular the supposedly warm-water bryozoans. While measurement of the $\delta^{18}O$ of skeletal carbonate would be sufficient to determine whether any taxa lived under markedly warmer conditions, it would be gratifying to 'fix' temperatures by allying this with techniques for accurately

estimating water $\delta^{18}O$. 'Clumped isotope' (Δ_{47}) analysis (e.g., Winkelstern et al., 2017) and measurement of the $\delta^{18}O$ of homeotherm phosphate (e.g., Walliser et al., 2015) are propitious methods. Finally, it would be worth applying geochemical approaches (e.g., foraminiferal Mg/Ca, alkenone unsaturation; Dowsett and Robinson, 2009) to material of pelagic origin to test the accuracy of the sea-surface temperatures deduced from seafloor data herein.

Acknowledgements

We thank James Rolfe and Michael Maus for assistance with isotopic analysis; the Sedgwick Museum for providing Coralline Crag specimens; Sharon Richardson for drafting Fig. 1; Peter Balson, Tony Dickson, Robert Marquet and Adrian Wood for helpful discussions during the course of the research; and the reviewers for detailed and constructive comments which greatly improved the paper. Funding: this work was partially supported by a PhD studentship award to AMV under the University Funding Initiative of the British Geological Survey (BUFI S157); and a grant of analytical services to ALAJ through the NERC Isotope Geoscience Facilities Steering Committee (IP-1155-1109).

References

Arthur, M.A., Williams, D.F., Jones, D.S., 1983. Seasonal temperature-salinity changes and thermocline development in the mid-Atlantic Bight as recorded by the isotopic composition of bivalves. Geology 11, 655–659, doi: 10.1130/0091-7613(1983)11<655:STCATD>2.0.CO;2.

Bachem, P.E., Risebrobakken, B., McClymont, E.L., 2016. Sea surface temperature variability in the Norwegian Sea during the late Pliocene linked to subpolar gyre

strength and radiative forcing. Earth. Planet. Sci. Lett. 446, 113–122, doi: 10.1016/j.epsl.2016.04.024.

Balson, P.S., 1983. Temperate, meteoric diagenesis of Pliocene skeletal carbonates from eastern England. J. Geol. Soc. Lond. 140, 377–385, doi: 10.1144/gsjgs.140.3.0377.

Balson, P.S., 1992. Tertiary. In: Cameron, T.D.J., Crosby, A., Balson, P.S., Jeffery, D.H., Lott, G.K. (Eds.), The Geology of the Southern North Sea. Her Majesty's Stationery Office, London, pp. 91–100.

Balson, P.S., 1999. The Coralline Crag. In: Daley, B., Balson, P.S. (Eds.), British Tertiary Stratigraphy. Geological Conservation Review Series 15. The Joint Nature Conservation Committee, Peterborough, pp. 253–288.

Balson, P.S., Taylor, P.D., 1982. Palaeobiology and systematics of large cyclostome bryozoans from the Pliocene Coralline Crag of Suffolk. Palaeontology 25, 529–554.

Balson, P.S., Mathers, S.J., Zalasiewicz, J.A., 1993. The lithostratigraphy of the Coralline Crag (Pliocene) of Suffolk. Proc. Geol. Assoc. 104, 59–70.

Barbin, V., Ramseyer, K., Debemay, J.P., Schein, E., Roux, M., Decrouez, D., 1991. Cathodoluminescence of recent biogenic carbonates: an environmental and ontogenetic fingerprint. Geol. Mag. 128, 19–26, doi: 10.1017/S001675680001801X.

Bemis, B.E., Spero, H.J., Bijma, J., Lea, D.W., 1998. Reevaluation of the oxygen isotopic composition of planktonic foraminifera: Experimental results and revised paleotemperature equations. Paleoceanography 13, 150–160, doi: 10.1029/98PA00070.

Bieler, R., Mikkelsen, P.M., Collins, T.M., Glover, E.A., González, V.L., Graf, D.L., Harper, E.M., Healy, J., Kawauchi, G.Y., Sharma, P.P., Staubach, S. Strong, E E., Taylor, J.D., Tëmkin, I. Zardus, J.D., Clark, S., Guzmán, A., McIntyre, E., Sharp, P., Giribet, G., 2014. Investigating the Bivalve Tree of Life—an exemplar-based approach

combining molecular and novel morphological characters. Invert. Syst. 28, 32–115, doi: 10.1071/IS13010.

Bishop, J.D.D., 1987. Type and figured material from the 'Pliocene Bryozoa of the Low Countries' (Lagaaij, 1952) in the collections of the Royal Belgian Institute of Natural Sciences. Doc Trav, Inst. R. Sci. Nat. Belg. 37, 1–36.

Bishop, J.D.D., 1994. The genera *Cribrilina* and *Collarina* (Bryozoa, Cheilostomatida) in the British Isles and North Sea Basin, Pliocene to present day. Zool. Scr. 23, 225–249, doi: 10.1111/j.1463-6409.1994.tb00387.x.

Bishop, J.D.D., Hayward, P.J. 1989. SEM Atlas of type and figured material from Robert Lagaaij's 'The Pliocene Bryozoa of the Low Countries' (1952). Mededelingen Rijks Geologische Dienst 43, 1–64.

Broom, M.J., Mason, J., 1978. Growth and spawning in the pectinid *Chlamys opercularis* in relation to temperature and phytoplankton concentration. Mar. Biol. 47, 277–285, doi: 10.1007/BF00541005.

Buchardt, B., Símonarson, L.A., 2003. Isotope palaeotemperatures from the Tjörnes beds in Iceland. Palaeogeog. Palaeoclimat. Palaeoecol. 189, p. 71–95, doi: 10.1016/S0031-0182(02)00594-1.

Busk, G., 1859. A monograph of the fossil Polyzoa of the Crag. The Palaeontographical Society, London, 136 pp.

Cadée, G.C., 1982. Notes on Bryozoa 2. *Membraniporella gigas* n. sp., and some other additions to the British Coralline Crag bryozoan fauna. Mededelingen van de Werkgroep voor Tertiaire en Kwartaire Geologie 19, 127–140.

Carpenter, S.J., Lohmann, K.C., 1995. $d^{18}O$ and $d^{13}C$ values of modern brachiopod shells: Geochim. Cosmochim. Acta 59, 3749–3764, doi: 10.1016/0016-7037(95)00291-7.

Casella, L.A., Griesshaber, E., Yin, X., Ziegler, A., Mavromatis, V., Müller, D., Ritter, A.-C., Hippler, D., Harper, E.M., Dietzel, M., Immenhauser, A., Schöne, B.R., Angiolini, L., Schmahl, W.W., 2017. Experimental diagenesis: insights into aragonite to calcite transformation of *Arctica islandica* shells by hydrothermal treatment, Biogeosci. 14, 1461–1492, doi:10.5194/bg-14-1461-2017.

Charlesworth, E., 1835. Observations on the Crag formation and its organic remains; with a view to establish a division of the Tertiary strata overlying the London Clay in Suffolk. Lond. Edinb. Phil. Mag. series 3, 7, 81–94.

Cheetham, A.H. 1967., Paleoclimatic evidence of the bryozoan *Metraradotos.* Trans. GCAGS 17, 400–407.

Claypool, G.E., Threlkeld, C.N., 1983. Anoxic diagenesis and methane generation in sediments of the Blake outer ridge DSDP Site 533, Leg 76. In: Initial Reports of the Deep Sea Drilling Project 76. U.S. Government Printing Office, Washington, D.C. , pp. 391–402.

Dearing Crampton-Flood, E., Peterse, F., Munsterman, D., Sinninghe Damsté, J.S., 2018, Using tetraether lipids archived in North Sea Basin sediments to extract North Western European Pliocene continental air temperatures. Earth and Plan. Sci. Lett. 490, 193–205, doi: 10.1016/j.epsl.2018.03.030.

De Schepper, S., Head, M.J., Louwye, S., 2009. Pliocene dinoflagellate cyst stratigraphy, palaeoecology and sequence stratigraphy of the Tunnel-Canal dock, Belgium. Geol. Mag. 146, 92–112, doi: 10.1017/S0016756808005438.

De Schepper, S., Groeneveld, J., Naafs, B.D.A., Van Renterghem, C., Hennissen, J., Head, M.J., Louwye, S., Fabian, K., 2013. Northern hemisphere glaciation during the globally warm early Late Pliocene. PLoS ONE 8, no. e81508, doi: 10.1371/journal.pone.0081508.

De Schepper, S., Gibbard, P.L., Salzmann, U., Ehlers, J., 2014. A global synthesis of the marine and terrestrial evidence for glaciation during the Pliocene Epoch. Earth Sci. Revs. 135, 83–102, doi: 10.1016/j.earscirev.2014.04.003.

Dowsett, H.J., Robinson, M.M., 2009. Mid-Pliocene equatorial Pacific sea surface temperature reconstruction: a multi-proxy perspective. Phil. Trans. Roy. Soc. A 367, 109–125, doi: 10.1098/rsta.2008.0206.

Dowsett, H.J., Robinson, M.M., Haywood, A.M., Hill, D.J., Dolan, A.M., Stoll, D.K., Chan, W.-L., Abe-Ouchi, A., Chandler, M.A., Rosenbloom, N.A., Otto-Bliesner, B.L., Bragg, F.J, Lunt, D.J., Foley, K.M., Riesselman, C.R., 2012. Assessing confidence in Pliocene sea surface temperatures to evaluate predictive models. Nature Clim. Change 2, 365–371, doi: 10.1038/NCLIMATE1455.

Dowsett, H.J., Foley, K.M., Stoll, D.K., Chandler, M.A., Sohl, L.E., Bentsen, M., Otto-Bliesner, B.L., Bragg, F.J., Chan, W.-L., Contoux, C., Dolan, A.M., Haywood, A.M., Jonas, J.A., Jost, A., Kamae, Y., Lohmann, G., Lunt, D.J., Nisancioglu, K.H., Abe-Ouchi, A., Ramstein, G., Riesselman, C.R., Robinson, M.M., Rosenbloom, N.A., Salzmann, U., Stepanek, C., Strother, S.L., Ueda, H., Yan, Q., Zhang, Z., 2013. Sea surface temperature of the mid-Piacenzian ocean: a data-model comparison. Sci. Rep. 3, 2013, doi: 10.1038/srep02013.

Encyclopaedia of Life. http://www.eol.org/ (last accessed 29th July 2017).

Füllenbach, C.S., Schöne, B.R., Mertz-Kraus., R, 2015. Strontium/lithium ratio in shells of *Cerastoderma edule* (Bivalvia) - A new potential temperature proxy for brackish environments. Chem. Geol. 417, 341–355, doi: 10.1016/j.chemgeo.2015.10.030.

Gibbard, P.L., Head, M.J., Walker, M.J.C., 2010. Subcommission on Quaternary stratigraphy. Formal ratification of the Quaternary System/Period and the Pleistocene

Series/Epoch with a base at 2.58 Ma. J. Quaternary Sci. 25, 96–102, doi: . 10.1002/jqs.1338

Gladenkov, Yu.B., Pokrovskiy, B.G., 1980. Oxygen-isotope composition of bivalve shells and climatic change in the North Atlantic region in late Cenozoic time. Int. Geol. Rev. 22, 826–830.

Goewert, A.E., Surge, D., 2008. Seasonality and growth patterns using isotope sclerochronology in shells of the Pliocene scallop *Chesapecten madisonius*. Geo-Mar.Lett. 28, 327–338, doi: 10.1007/s00367-008-0113-7.

Gonfiantini, R., Stichler, W., Rozanski, K., 1995 Standards and intercomparison materials distributed by the International Atomic Energy Agency for stable isotope measurements, *in* International Atomic Energy Agency, Reference and Intercomparison Materials for Stable Isotopes of Light Elements: IAEA-TECDOC-825, Vienna, Austria, 13–29.

Grossman, E.L. and Ku, T., 1986. Oxygen and carbon isotope fractionation in biogenic aragonite: Temperature effects. Chem. Geol. (Isotope Geosci. Sect.) 59, 59–74, doi: 10.1016/0009-2541(86)90044-6.

Hall, C.A., Jr, 1964. Shallow-water marine climates and molluscan provinces. Ecology 45, 226–234.

Harmer, F.W., 1896. The southern character of the molluscan fauna of the Coralline Crag tested by an analysis of its more abundant and characteristic species. Geol. Mag. 33, 27–31.

Harmer, F.W., 1914–18. The Pliocene Mollusca of Great Britain, being supplementary to S.V. Wood's Monograph of the Crag Mollusca. Volume I. Mon. Pal. Soc. Lond. pp. 1–200 (1914), pp. 201–302 (1915), pp. 303–461 (1918).

Harmer, F.W., 1920–1925. The Pliocene Mollusca of Great Britain, being supplementary to S.V.Wood's Monograph of the Crag Mollusca. Volume II. Mon. Pal. Soc. Lond. pp. 485–562 (1920), pp. 653–704 (1921), pp. 705–856 (1923), pp. 857–900 (1925).

Head, M.J., 1993. Dinoflagellates, sporomorphs, and other palynomorphs from the upper Pliocene St. Erth Beds of Cornwall, southwestern England. J. Pal., 67, 1–62.

Head, M.J., 1997. Thermophilic dinoflagellate assemblages from the mid-Pliocene of Eastern England. J. Paleont. 71, 165–193, doi: 10.1017/S0022336000039123.

Head, M.J., 1998. Marine environmental change in the Pliocene and Early Pleistocene of eastern England: the dinoflagellate evidence reviewed. Mededelingen Nederlands Inst. Toegepaste Geowetenschappen 60, 199–225.

Hickson, J.A., Johnson, A.L.A., Heaton, T.H.E., Balson, P.S., 1999. The shell of the Queen Scallop *Aequipecten opercularis* (L.) as a promising tool for palaeoenvironmental reconstruction: evidence and reasons for equilibrium stable-isotope incorporation. Palaeogeogr. Palaeoclimatol. Palaeoecol. 154, 325–337, doi: 10.1016/S0031-0182(99)00120-0.

Hickson, J.A., Johnson, A.L.A., Heaton, T.H.E., Balson, P.S., 2000. Late Holocene environment of the southern North Sea from the stable isotopic composition of Queen Scallop shells. Palaeont. Electr., 3, iss. 2, art. 3, 11 pp, http://palaeo-electronica.org/2000_2/scallop/issue2_00.htm.

Huber, M., 2010. Compendium of bivalves: a full-color guide to 3,300 of the world's marine bivalves: a status on Bivalvia after 250 years of research. ConchBooks, Hackenheim, 501 pp.

Jeffreys, J.G., 1871. On the adult form in the genera *Cypræa* and *Ringicula*, and in certain species of the genus *Astarte*. Ann. Mag. Nat. Hist. 7(39), 245–245.

Johnson, A.L.A., Hickson, J.A., Swan, J., Brown, M.R., Heaton, T.H.E., Chenery, S., Balson, P.S., 2000, The queen scallop *Aequipecten opercularis*: a new source of information on late Cenozoic marine environments in Europe. In: Harper, E.M., Taylor, J.D., Crame, J.A. (Eds.), Evolutionary Biology of the Bivalvia, Volume 177, Geological Society of London, Spec. Publ., pp. 425–439, doi: 10.1144/GSL.SP.2000.177.01.28

Johnson, A.L.A., Hickson, J.A., Bird, A., Schöne, B.R., Balson, P.S., Heaton, T.H.E., Williams, M., 2009. Comparative sclerochronology of modern and mid-Pliocene (c. 3.5 Ma) *Aequipecten opercularis* (Mollusca, Bivalvia): an insight into past and future climate change in the north-east Atlantic region. Palaeogeogr. Palaeoclimatol. Palaeoecol. 284, 164–179, doi: 10.1016/j.palaeo.2009.09.022.

Johnson, A.L.A., Valentine, A., Leng, M.J., Sloane, H.J., Schöne, B.R., Balson, P.S., 2017. Isotopic temperatures from the Early and Mid-Pliocene of the US Middle Atlantic Coastal Plain, and their implications for the cause of regional marine climate change. PALAIOS 32, 250–269, doi: 10.2110/palo.2016.080.

Jones, D.S., Quitmyer, I.R., 1996. Marking time with bivalve shells: Oxygen isotopes and season of annual increment formation. PALAIOS 11, 340–346, doi: 10.2307/3515244.

Kim, S.T., O'Neil, J.R., 1997. Equilibrium and nonequilibrium oxygen isotope effects in synthetic carbonates. Geochim. Cosmochim. Acta 61, 3461–3475, doi: 10.1016/S0016-7037(97)00169-5 .

Kim, S.-T., O'Neil, J.R., Hillaire-Marcel, C., Mucci, A., 2007. Oxygen isotope fractionation between synthetic aragonite and water: Influence of temperature and Mg^{2+} concentration. Geochim. Cosmochim. Acta 71, 4704–4715, doi: 10.1016/j.gca.2007.04.019.

Krantz, D.E., 1990. Mollusk-isotope records of Plio-Pleistocene marine paleoclimate, U.S. Middle Atlantic Coastal Plain. PALAIOS 5, 317–335, doi: 10.2307/3514888.

Krantz, D.E., Williams, D.F., Jones, D.S., 1987. Ecological and paleoenvironmental information using stable isotope profiles from living and fossil molluscs. Palaeogeogr. Palaeoclimatol. Palaeoecol. 58, 249–266, doi: 10.1016/0031-0182(87)90064-2.

Lagaaij, R., 1963. *Cupuladria canariensis* (Busk) - portrait of a bryozoan. Palaeontol. 6, 172–217.

Long, P.E., Zalasiewicz, J.A., 2011. The molluscan fauna of the Coralline Crag (Pliocene, Zanclean) at Raydon Hall, Suffolk, UK. Palaeoecological significance reassessed. Palaeogeogr. Palaeoclimatol. Palaeoecol. 309, 53–72, doi: 10.1016/j.palaeo.2011.05.039.

Long, P.E., Zalasiewicz, J.A., 2012. Why look again at the Coralline Crag? Mainly a molluscan story. In: Dixon, R, (Ed.), A celebration of Suffolk geology, GeoSuffolk 10th Anniversary Volume, GeoSuffolk, Ipswich, pp. 149–161.

Mann, R., Wolf, C.C., 1983, Swimming behaviour of larvae of the ocean quahog *Arctica islandica* in response to pressure and temperature. Mar. Ecol.—Prog. Ser. 13, 211–218, doi: 10.3354/meps013211.

Marine Bivalve Shells of the British Isles. http://naturalhistory.museumwales.ac.uk/britishbivalves/ (last accessed 29th July 2017).

Marine Life Information Network. http://www.marlin.ac.uk/ (last accessed 29th July 2017).

Marquet, R., 2002. The Neogene Amphineura and Bivalvia (Protobranchia and Pteriomorphia) from Kallo and Doel (Oost-Vlaanderen, Belgium). Palaeontos 2, 1–99.

Marquet, R., 2005. The Neogene Bivalvia (Heterodonta and Anomalodesmata) and Scaphopoda from Kallo and Doel (Oost Vlaanderen, Belgium). Palaeontos 6, 1–142.

Marquet, R., Herman, J., 2009. The stratigraphy of the Pliocene in Belgium. Palaeofocus 2, 1–39.

McKinney, C.R., McCrea, J.M., Epstein, S., Allen, H.A., Urey, H.C., 1950. Improvements in mass spectrometers for the measurement of small differences in isotope abundance ratios. Rev. Sci. Instrum. 21, 724–730.

Murray, J.W., 1987. Benthonic foraminiferal assemblages: criteria for the distinction of temperate and subtropical carbonate environments. In: Hart, M.B., (Ed.), Micropalaeontology of Carbonate Environments, British Micropalaeontological Society, Spec. Publ., The Geological Society, London, pp. 9–20.

Murray, J.W., 1992. Palaeogene and Neogene. In: Cope, J.C.W., Ingham, J.K., Rawson, P.F. (Eds.), Atlas of palaeogeography and lithofacies. Mem. Geol. Soc., Lond. 13, 141–147.

NOAA (US Department of Commerce, National Oceanic and Atmospheric Administration), 1994. NODC (Levitus) World Ocean Atlas: Ocean Temperature: Monthly Long Term Mean (http://www.cdc.noaa.gov/cgi-bin/db_search/DBSearch.pl?Dataset=NODC+(Levitus)+World+Ocean+Atlas&Variable=Ocean+temperature; last accessed 22nd July 2017).

Ocean Biogeographic Information System. http://www.iobis.org/ (last accessed 29th July 2017).

O'Neil, J.R., Clayton, R.N., Mayeda, T.K., 1969. Oxygen isotope fractionation in divalent metal carbonates. J. Chem. Phys. 51, 5547–5558.

Pierre, C., 1999. The oxygen and carbon isotope distribution in the Mediterranean water masses. Mar. Geol. 153, 41–55, doi: 10.1016/S0025-3227(98)00090-5.

Presley, B.J., Kaplan, I.R., 1970. Interstitial water chemistry: Deep Sea Drilling Project. Leg 4. In: Initial Reports of the Deep Sea Drilling Project, 4. U.S. Government Printing Office, Washington, D.C. pp. 415–430.

Prestwich, J., 1871. On the structure of the Crag-beds of Suffolk and Norfolk with some observations on their organic remains. Part I. The Coralline Crag of Suffolk. Q. J. Geol. Soc. Lond. 27, 115–146.

Raffi, S., Stanley, S.M., Marasti, R., 1985. Biogeographic patterns and Plio-Pleistocene extinction of Bivalvia in the Mediterranean and southern North Sea. Paleobiol. 11, 368–388, doi:.

Richardson, C.A., 2001. Molluscs as archives of environmental change. In: Gibson, R.N., Barnes, M., Atkinson, R.J.A. (Eds.), Oceanography and marine biology: an Annual Review 2001, Vol. 39, Taylor and Francis, Oxford, pp. 103–164.

Richardson, C.A., Crisp, D.J., Runham, N.W., 1979. Tidally deposited growth bands in the shell of the common cockle *Cerastderma edule* (L.). Malacologia 18, 227–290.

Royer, C., Thébault, J., Chauvaud, L., Olivier, F., 2013. Structural analysis and paleoenvironmental potential of dog cockle shells (*Glycymeris glycymeris*) in Brittany, northwest France. Palaeogeogr. Palaeoclimatol. Palaeoecol. 373, 123–132, doi: 10.1016/j.palaeo.2012.01.033.

Schöne, B.R., Fiebig, J., Pfeiffer, M., Gleß, R., Hickson, J., Johnson, A.L.A., Dreyer, W., Oschmann, W., 2005a. Climate records from a bivalved Methuselah (*Arctica islandica*, Mollusca; Iceland). Palaeogeogr. Palaeoclimatol. Palaeoecol. 228, 130–148, doi: 10.1016/j.palaeo.2005.03.049.

Schoene, B.R., Dunca, E., Fiebig, J., Pfeiffer, M., 2005b. Mutvei's solution: An ideal agent for resolving microgrowth structures of biogenic carbonates. Palaeogeogr. Palaeoclimatol. Palaeoecol. 228, 149–166, doi: 10.1016/j.palaeo.2005.03.054.

Shackleton, N.J., 1974. Attainment of isotopic equilibrium between ocean water and the benthonic foraminifera genus *Uvigerina*: Isotopic changes in the ocean during the last glacial. Cent. Nat. Rech., Sci. Colloq. Int. 219, 203–209.

Taylor, P.D., Taylor, A.B., 2012. Bryozoans from the Pliocene Coralline Crag of Suffolk: a brief review, in: Dixon, R, (Ed.), A celebration of Suffolk geology, GeoSuffolk 10th Anniversary Volume, GeoSuffolk, Ipswich, pp. 163–173.

Valentine, A., Johnson, A.L.A., Leng, M.J., Sloane, H.J., Balson, P.S., 2011. Isotopic evidence of cool winter conditions in the mid-Piacenzian (Pliocene) of the southern North Sea Basin. Palaeogeogr. Palaeoclimatol. Palaeoecol. 309, 9–16, doi: 10.1016/j.palaeo.2011.05.015.

Verhoeven, K., Louwye, S., Eiríksson, J., De Schepper, S., 2011. A new age model for the Pliocene-Pleistocene Tjörnes section on Iceland: Its implications for the timing of North Atlantic-Pacific palaeoceanographic pathways. Palaeogeogr. Palaeoclimatol. Palaeoecol. 309, 33–52, doi: 10.1016/j.palaeo.2011.04.001.

Walliser, E.O., Schöne, B.R., Tütken, T., Zirkel, J., Grimm, K.I., and Pross, J., 2015. The bivalve *Glycymeris planicostalis* as a high-resolution paleoclimate archive for the Rupelian (Early Oligocene) of central Europe. Clim. Past 11, 653–668, doi: 10.5194/cp-11-653-2015.

Wanamaker, A.D., Kreutz, K.J., Schone, B.R., Introne, D.S., 2011. Gulf of Maine shells reveal changes in seawater temperature seasonality during the Medieval Climate Anomaly and the Little Ice Age, Palaeogeogr. Palaeoclimatol. Palaeoecology, 302, 43–51, doi: 10.1016/j.palaeo.2010.06.005.

Ward, L.W., Bailey R.H., Carter, J.G., 1991. Pliocene and early Pleistocene stratigraphy, depositional history, and molluscan paleobiogeography of the Coastal Plain. In:

Horton, J.W., Jr., Zullo, V.A. (Eds.), The Geology of the Carolinas. University of Tennessee Press, Knoxville, Tennessee, pp. 274–289.

Williams, A., 1990. Brachiopoda and Bryozoa. In: Carter, J.G. (Ed.), Skeletal Biomineralization; Patterns, Processes and Evolutionary Trends. Vol. 2. Atlas and Index. Van Nostrand Reinhold, New York, pp. 57–61 (pls. 141–156).

Williams, M., Haywood, A.M., Harper, E.M., Johnson, A.L.A., Knowles, T., Leng, M.J., Lunt, D.J., Okamura, B., Taylor, P.D., Zalasiewicz, J., 2009. Pliocene climate and seasonality in North Atlantic shelf seas. Phil. Trans. Roy. Soc. A 367, 85–108, doi: 10.1098/rsta.2008.0224.

Winkelstern, I., Surge, D., Hudley, J.W., 2013. Multiproxy sclerochronological evidence for Plio-Pleistocene regional warmth: United States Mid-Atlantic Coastal Plain. PALAIOS, 28, 649–660, doi: 10.2110/palo.2013.p13-010r.

Winkelstern, I. Z., Rowe, M.P., Lohmann, K.C., Defliese, W.F., Petersen, S.V., Brewer , A.W., 2017. Meltwater pulse recorded in Last Interglacial mollusk shells from Bermuda, Paleoceanogr. 32, doi: 10.1002/2016PA003014.

Witbaard, R., 1997. Tree of the sea: the use of the internal growth lines in the shell of "*Arctica islandica*" (Bivalvia, Mollusca) for the retrospective assessment of marine environmental change. PhD thesis, University of Groningen, The Netherlands, 149 pp.

Witbaard, R., Bergman, M.J.N., 2003. The distribution and population structure of the bivalve *Arctica islandica* L. in the North Sea: what possible factors are involved? J. Sea Res. 50, 11–25, doi: 10.1016/S1385-1101(03)00039-X.

Witbaard, R., Duineveld, G.C.A., De Wilde, P.A.W.J., 1997. A long-term growth record derived from *Arctica islandica* (Mollusca, Bivalvia) from the Fladen Ground

(northern North Sea): J. Mar. Biol. Assoc., UK. 77, 801–816, doi: 10.1017/S0025315400036201.

Wood, A.M., Whatley, R.C., Cronin, T.M., Holtz, T., 1993. Pliocene palaeotemperature reconstruction for the southern North Sea based on Ostracoda. Quat. Sci. Rev. 12, 747–767, doi: 10.1016/0277-3791(93)90015-E.

Wood, A.M., Wilkinson, I.P., Maybury, C.A., Whatley, R.C., 2009. Neogene. In: Whittaker, J.E., Hart, M.B. (Eds.), Ostracods in British Stratigraphy. The Micropalaeontological Society, Spec. Publ., The Geological Society, London, pp. 411–446.

Wood, S.V., 1848. A monograph of the Crag Mollusca, or, descriptions of shells from the Middle and Upper Tertiaries of the east of England. Part 1. Univalves. Palaeontogr. Soc. Monogr., pp. i–xi + 1–208, pls. 1–21.

Wood, S.V., 1851–61. A monograph of the Crag Mollusca, or, descriptions of shells from the Middle and Upper Tertiaries of the east of England. Part 2. Bivalves. Palaeontogr. Soc. Monogr., pp. 1–150, pls. 1–12 (1851), pp. 151–216, pls. 13–20 (1853), pp. 217–342, pls. 21–31(1857), note 1–2 (1861).

Wood, S.V., 1872–74. Supplement to the monograph of the Crag Mollusca, with descriptions of shells from the Upper Tertiaries of the east of England. Univalves and Bivalves. Palaeontogr. Soc. Monogr., pp. i–xxxi + 1–231.

Wood, S.V., 1879. Second supplement to the monograph of the Crag Mollusca, with descriptions of shells from the Upper Tertiaries of the east of England. Palaeontogr. Soc. Monogr., pp. i–ii + 1–58.

Wood, S.V., 1882. Third supplement to the Crag Mollusca comprising Testacea from the Upper Tertiaries of the East of England. Univalves and bivalves. Palaeontogr. Soc. Monogr., 1–24.

Wood, S.V., 1882. Third supplement to the Crag Mollusca comprising Testacea from the Upper Tertiaries of the East of England. Univalves and bivalves. Palaeontogr. Soc. Monogr. 1–24.

World Register of Marine Species. http://marinespecies.org/ (last accessed 29th July 2017).

Wright, J., Colling, A., Park, A., 1999. Waves, Tides and Shallow-Water Processes. Butterworth Heinemann/The Open University, Milton Keynes, 227 pp.

Zhao, L., Walliser, E.O., Mertz-Kraus, R., Schöne, B.R., 2017. Unionid shells (*Hyriopsis cumingii*) record manganese cycling at the sediment-water interface in a shallow eutrophic lake in China (Lake Taihu). Palaeogeogr. Palaeoclimatol. Palaeoecol. 484, 97–108, doi: 10.1016/j.palaeo.2017.03.010.

FIGURE CAPTIONS

Fig. 1. Position of main onshore outcrop of the Coralline Crag Formation in Suffolk, East Anglia, eastern England (1 and inset), locations of other sequences in north-west Europe mentioned in the text (2–4), and Pliocene paleogeography of the area (adapted from Murray, 1992, map NG1). Sea is blue (beige over current land); brown is land (pink over current sea). The St Erth sequence, England (2), was dated by Head (1993) to within the Gelasian, formerly the uppermost stage of the Pliocene but now placed in the Pleistocene following redefinition of the Pliocene/Pleistocene boundary (Gibbard et al., 2010). The borehole sequence at Ouwerkerk, The Netherlands (3), includes Pliocene material (e.g., Valentine et al., 2011) but is only one of many subsurface occurrences of Pliocene deposits throughout The Netherlands (Marquet and Herman, 2009). Dock construction at Antwerp, Belgium (4), provided temporary exposures of the Pliocene sequence there (Marquet and Herman, 2009). The outliers of Coralline Crag mentioned in the text are not shown; they extend the area of

occurrence of the formation less far (27 km west-south-west of the main onshore outcrop) than stated by Johnson et al. (2009).

Fig. 2. Stratigraphy of the Coralline Crag Formation in relation to sequences on the eastern side of the southern North Sea (Belgium) and western side of the North Atlantic (Virginia and N. Carolina, USA). Amended from Johnson et al. (2017, fig. 1) to take account of the evidence in De Schepper et al. (2009) that the Coralline Crag Formation has no equivalent in the Belgian sequence, being younger than the Kattendijk Formation and older than the Lillo Formation. Wood et al. (2009), however, consider that the Luchtbal Sands Member of the Lillo Formation is age-equivalent to the Coralline Crag Formation. Ages in Ma. MPWP = Mid-Piacenzian Warm Period. Asterisks indicate units for which there are existing isotopic paleotemperature determinations (Krantz 1990; Goewert and Surge, 2008; Johnson et al., 2009, 2017; Williams et al., 2009; Valentine et al., 2011; Winkelstern et al., 2013).

Fig. 3. Examples of *Aequipecten opercularis* (A, SM XXXXXX; AeO3), *Talochlamys multistriata* (B, SM XXXXXX; CV1), *Cardites squamulosa ampla* (C, SM TN552.5.1.2), *Astarte gracilis* (E, SM XXXXXX; AG5), *Lucinoma borealis* (F, SM XXXXXX; PB4), *Spisula arcuata* (G, SM XXXXXX; SA) and *Ringicula buccinea* (H, SM TN4187.1) from the Ramsholt Member, Coralline Crag Formation, and of *Cardites antiquatus* (D, SM XXXXXX; a close modern relative of *C. squamulosa ampla*) from the Mediterranean Sea off Almería, Spain. Note that the scales differ either side of the dashed line; scale bar = 10 mm in each portion. Pits from spot sampling are indicated by arrows in A, B, E, F. The greater prominence of commarginal lamellae in D compared to C is partly a reflection of preserved colour variation. Only the apertural region, representing 60-70% of the total shell height, is present in H.

Fig. 4. Annual growth increments in Coralline Crag specimens of *Arctica islandica* (A, B) and *Cardites squamulosa ampla* (C), and microgrowth (*c.* daily) increments in a modern specimen of *Aequipecten opercularis* from the Mediterranean Sea (D). A (54–61 mm from the origin of growth in *A. islandica* specimen 1) shows annual growth lines bounding annual increments in the outer (OL) and inner (IL) shell layers, together with the last four sample holes in the outer layer. B (17–21 mm from the origin of growth in *A. islandica* specimen 5) also shows annual growth lines in the outer and inner layers, together with the last four sample holes, but note that in this series from early ontogeny some of the sample holes transgress the boundary between the outer and inner layer. C (31–34 mm from the origin of growth, including the ventral edge of the shell, in *C. squamulosa ampla* specimen 7) shows annual growth lines in the outer and m+1 (outer part of the middle) layer, closely spaced in this late ontogenetic sequence (note that the outer layer, marked by reflexed growth lines, is often poorly preserved or lost nearer the origin of growth). D (18–26 mm from the origin of growth in a modern *A. opercularis* specimen from near Málaga, Spain; Muséum national d'Histoire naturelle, Paris, 21996) shows commarginal striae bounding microgrowth increments on the outer shell surface. A–C are images of acetate peels from sectioned shells (note that the white spots in C are bubbles on the acetate peel). Scale bars represent 1 mm in each part. dog = direction of extensional growth.

Fig. 5. Unaltered preservation of calcite (A, B) and aragonite (C-F) shell structures amongst isotopically investigated Coralline Crag species. A: foliated structure in *Talochlamys multistriata*; B: fibrous structure adjacent to a puncta in *Pliothyrina maxima*; C: homogeneous structure in *Arctica islandica*; D: crossed-lamellar structure in *Cardites squamulosa ampla*; E: complex crossed-lamellar structure in *Coripia corbis*; F: complex

crossed-lamellar structure in *Lucinoma borealis*. Note that the puncta in B is void of diagenetic calcite. A–C, E, F are fracture surfaces; D is a polished and etched surface. Scale bar = 10 μm for each part.

Fig. 6. Cathodoluminescence in specimens of *Cardites squamulosa ampla*. A: specimen 8, showing blue luminescence (indicating aragonite) in the inner and outer shell layers (seen in centre of image, with growth lines visible); sediment containing calcite (specks of orange luminescence) is seen to the left and resin to the right. B: specimen 7, showing blue luminescence in the inner and outer layers, and patches of dull orange luminescence in the middle layer; sediment containing large calcite grains (bright orange luminescence) is seen to the left and resin to the right (also infilling a cavity in the outer part of the outer layer). C: enlargement of the boxed area in B, showing faint transverse lines, representing the original crossed-lamellar shell structure, in an area of orange luminescence (colour brighter than in B due to enhancement of image to show shell structure). Scale bar = 1 mm for each part.

Fig. 7. A–D: Oxygen isotope (red line) and carbon isotope (black line) data from Coralline Crag specimens of *Arctica islandica*. Isotopic axis reversed so that lower values of $\delta^{18}O$ (representative of higher temperatures) plot towards the top. Dotted lines in A are for values from whole-year samples. E–H: Temperature profiles calculated using the oxygen isotope data in A–D, Equation 2 and values for $\delta^{18}O_{water}$ of –0.5‰ (blue lines), –0.2‰ (brown lines), +0.1‰ (orange lines) and +0.5‰ (yellow lines). The profiles for $\delta^{18}O_{water}$ of +0.1‰ (thicker lines) are preferred.

Fig. 8. A–D: Oxygen isotope (red line) and carbon isotope (black line) data from Coralline Crag specimens of *Cardites squamulosa ampla*. Isotopic axis reversed so that lower values of

$\delta^{18}O$ (representative of higher temperatures) plot towards the top. E–H: Temperature profiles calculated using the oxygen isotope data in A–D, Equation 2 and values for $\delta^{18}O_{water}$ of –0.5‰ (blue lines), –0.2‰ (brown lines), +0.1‰ (orange lines) and +0.5‰ (yellow lines). The profiles for $\delta^{18}O_{water}$ of +0.1‰ (thicker lines) are preferred.

Fig. 9. A, B: Oxygen isotope (red line), carbon isotope (black line) and microgrowth increment (blue line) data from Coralline Crag specimens of *Aequipecten opercularis*. Isotopic axis reversed so that lower values of $\delta^{18}O$ (representative of higher temperatures) plot towards the top. Distance from origin of growth measured as a straight line (not around the shell periphery) along the axis of maximum growth; increment size measured in the same direction. Thin, dashed blue lines = raw increment data; thicker, continuous blue lines = five-point averages. C, D: Temperature profiles calculated using the oxygen isotope data in A and B, Equation 1 and values for $\delta^{18}O_{water}$ of –0.5‰ (blue lines), –0.2‰ (brown lines), +0.1‰ (orange lines) and +0.5‰ (yellow lines). The profiles for $\delta^{18}O_{water}$ of +0.1‰ (thicker lines) are preferred.

Fig. 10. A, B: Oxygen isotope (red line) and carbon isotope (black line) data from Coralline Crag specimens of *Pliothyrina maxima*. Isotopic axis reversed so that lower values of $\delta^{18}O$ (representative of higher temperatures) plot towards the top. Distance from origin of growth measured as a straight line (not around the shell periphery) along the axis of maximum growth. C, D: Temperature profiles calculated using the oxygen isotope data in A and B, Equation 1 and values for $\delta^{18}O_{water}$ of –0.5‰ (blue lines), –0.2‰ (brown lines), +0.1‰ (orange lines) and +0.5‰ (yellow lines). The profiles for $\delta^{18}O_{water}$ of +0.1‰ (thicker lines) are preferred.

Fig. 11. A: Oxygen isotope (red line) and carbon isotope (black line) data from a Coralline Crag specimen of *Lucinoma borealis*. Isotopic axis reversed so that lower values of $\delta^{18}O$ (representative of higher temperatures) plot towards the top. Distance from origin of growth measured as a straight line (not around the shell periphery) along the axis of maximum growth. B: Temperature profile calculated using the oxygen isotope data in A, Equation 2 and values for $\delta^{18}O_{water}$ of –0.5‰ (blue line), –0.2‰ (brown line), +0.1‰ (orange line) and +0.5‰ (yellow line). The profile for $\delta^{18}O_{water}$ of +0.1‰ (thicker line) is preferred.

Fig. 12. Summary statistics for (A) summer $\delta^{18}O$ minima (pink) and winter $\delta^{18}O$ maxima (sea-green), and (B) all $\delta^{13}C$ values, from each of the ontogenetically sampled individuals and the taxa concerned as a whole. The plots show the range of values (thin lines with caps), mean (squares; sample number adjacent) and standard deviation (± 1σ; thick lines), with the taxic ('mean') data being the range, mean and standard deviation of individual means. Names of 'warm' taxa in red, 'cool' in blue, 'eurythermal' in mauve; taxa ordered as in Figure 14 (see caption for explanation); isotopic axes reversed to match Figures 7–11.

Fig. 13. Summary statistics for summer temperature maxima (pale red) and winter temperature minima (pale blue) from each of the ontogenetically sampled individuals and the taxa concerned as a whole, calculated using equation (1) or (2), as appropriate, and a water $\delta^{18}O$ value of +0.1‰. The plot shows the range of values (thin lines with caps), mean (squares; sample number adjacent) and standard deviation (± 1σ; thick lines) for maxima and minima, with the taxic ('mean') data being the range, mean and standard deviation of individual means. Names of 'warm' taxa in red, 'cool' in blue, 'eurythermal' in mauve. Winter and summer boundary temperatures between cool (C) and warm (W) temperate marine climate indicated.

Fig. 14. Temperatures (filled circles) calculated from spot and whole-shell $\delta^{18}O$ values, Equation (1) or (2), as appropriate, and values for water $\delta^{18}O$ of –0.5‰ (mid-blue), –0.2‰ (brown), +0.1‰ (orange) and +0.5‰ (yellow). Temperatures calculated using a water $\delta^{18}O$ of +0.1‰ (larger, orange filled circles) are preferred. Names of 'warm' taxa in red, 'cool' in blue, 'eurythermal' in mauve; number of specimens in parentheses. Bivalve taxa arranged in conventional order of families from left (Glycymeridae) to right (Arcticidae). Data arranged within taxa in order of increasing temperature to the right. Orange dotted lines signify mean of temperatures calculated using a water $\delta^{18}O$ of +0.1‰ for each taxon. Green dotted lines, and pale red and pale blue dashed lines, signify, respectively, overall mean, mean summer maximum and mean winter minimum temperatures from ontogenetic data (see sections 3.4.1–3.4.5 and Fig. 13). The grey dashed lines signify average summer maximum and average winter minimum temperatures (for both surface and seafloor) in the southern North Sea at present. Winter and summer boundary temperatures between cool (C) and warm (W) temperate marine climate indicated.

Figure 1

[Fig. 1 – for 1.5-column reproduction; colour required]

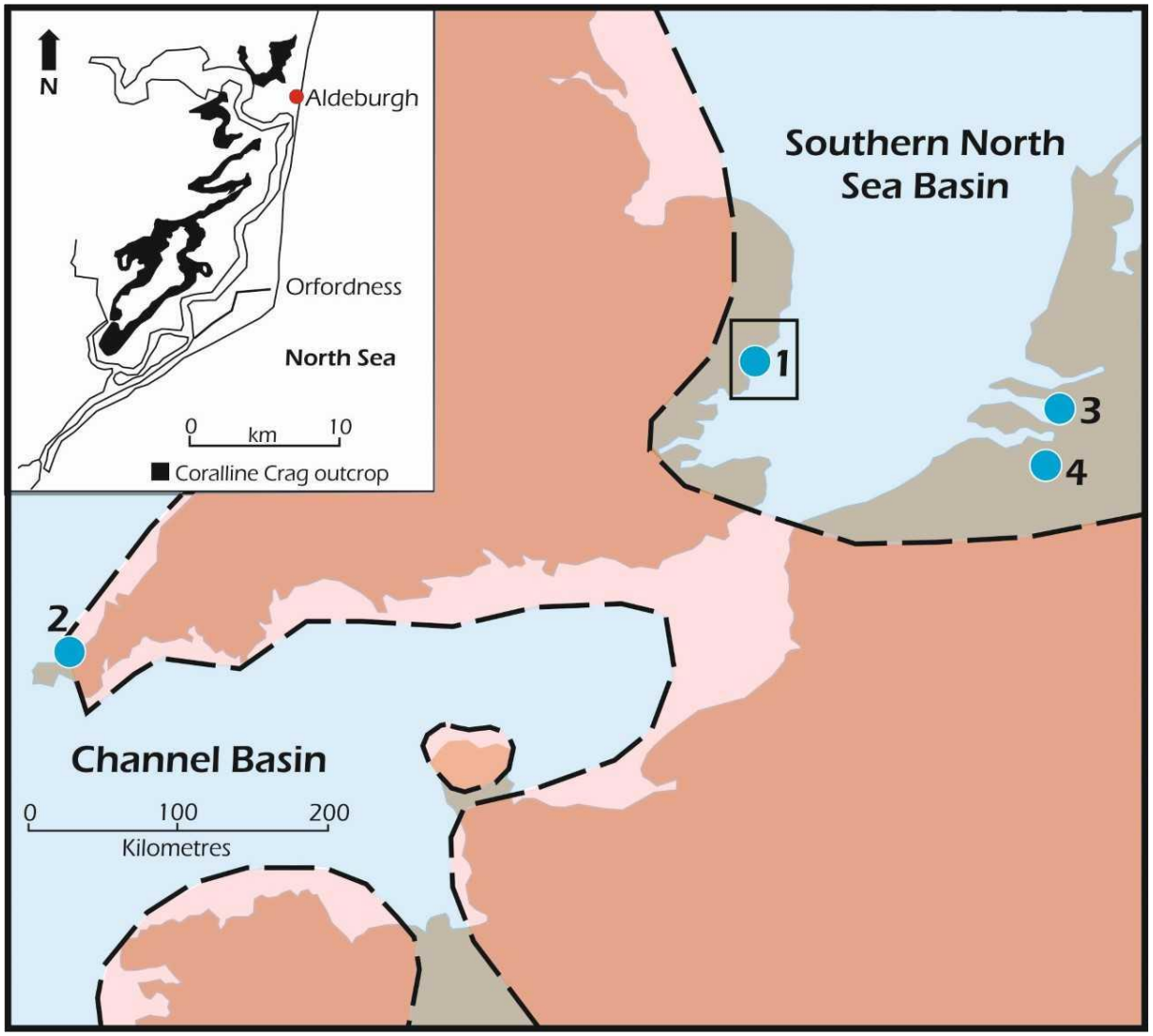

Figure 2

[Fig. 2 – for 1-column reproduction; colour required]

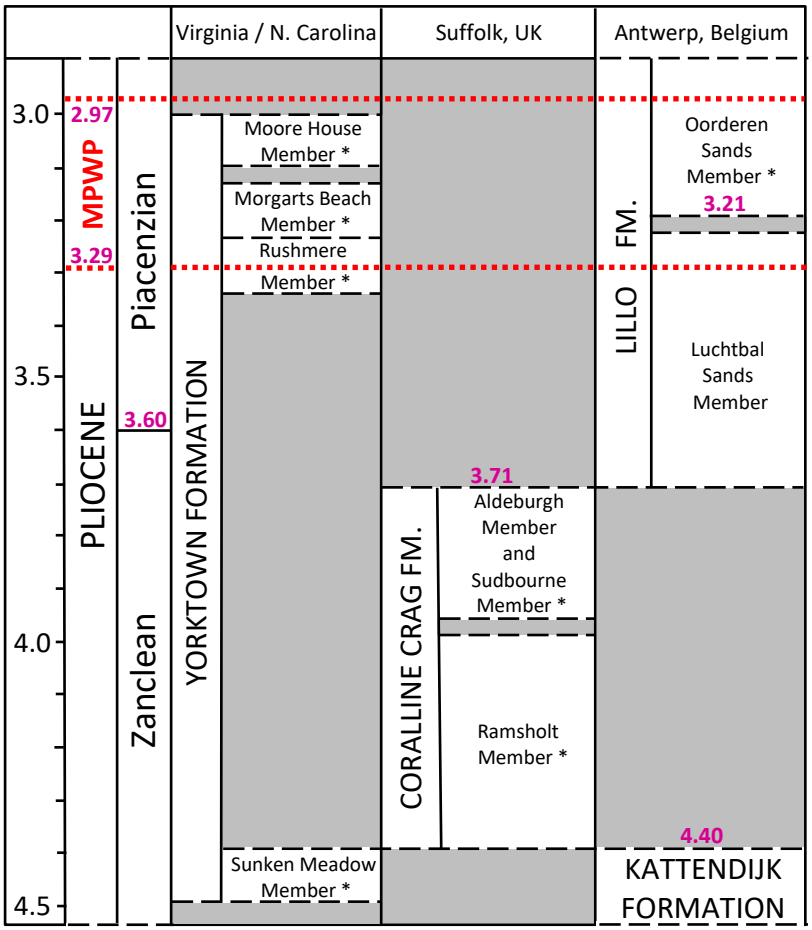

Figure 3

[Fig. 3 – for 1.5- or 2-column reproduction]

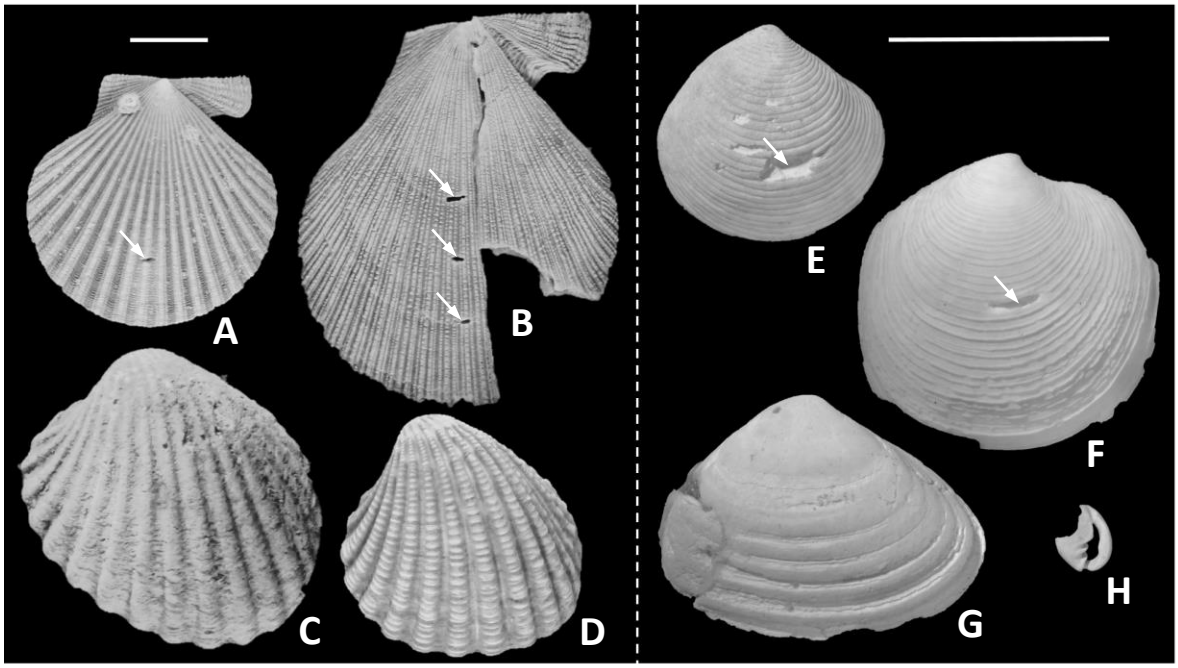

Figure 4

[Fig. 4 – for 1.5- or 2-column reproduction]

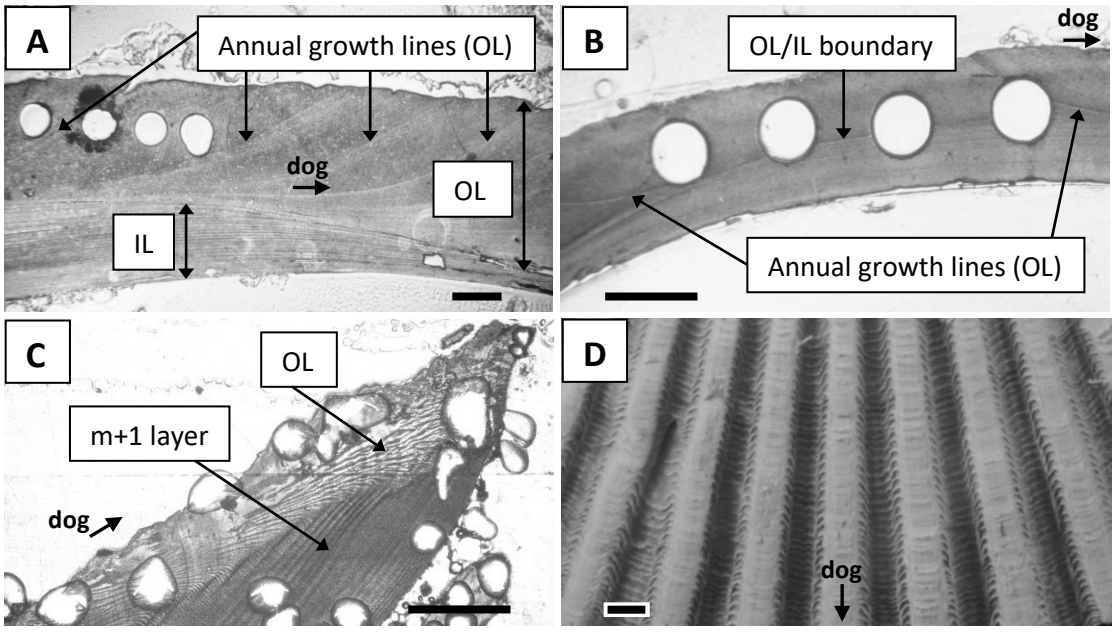

Figure 5

[Fig. 5 – for 1.5 or 2-column reproduction]

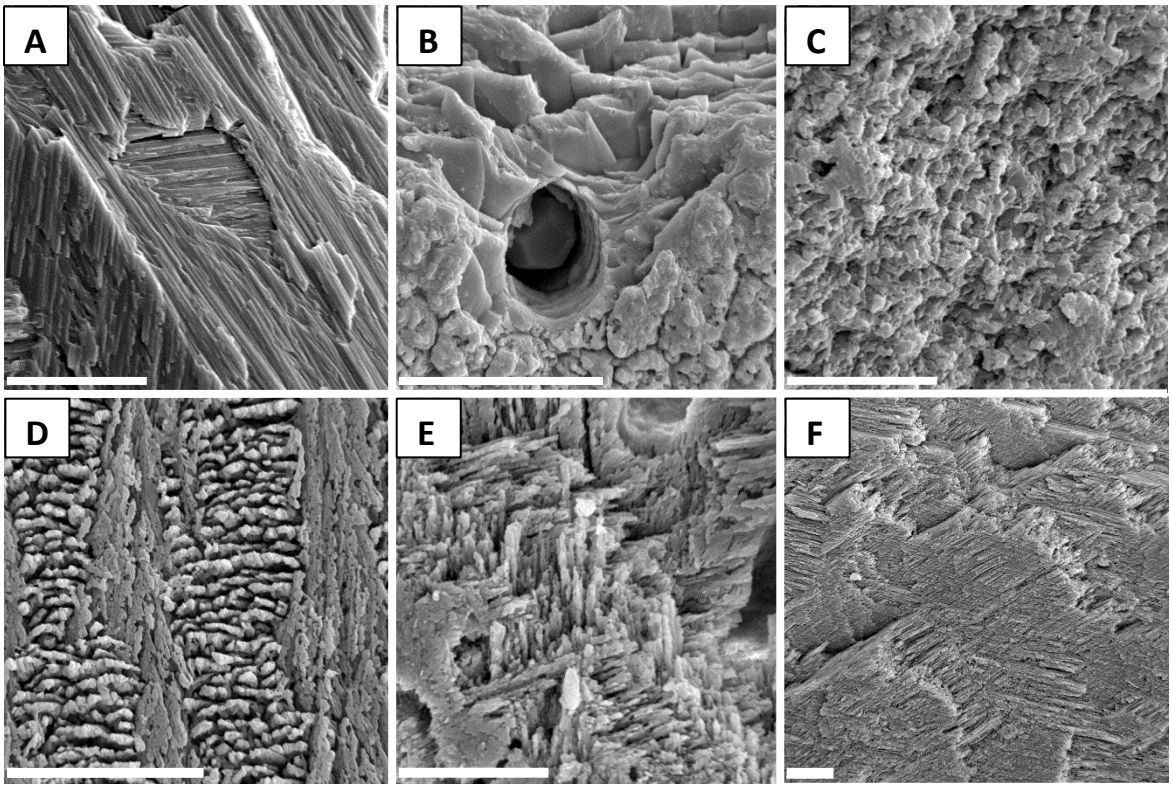

Figure 6

[Fig. 6 – for 2-column reproduction; colour required]

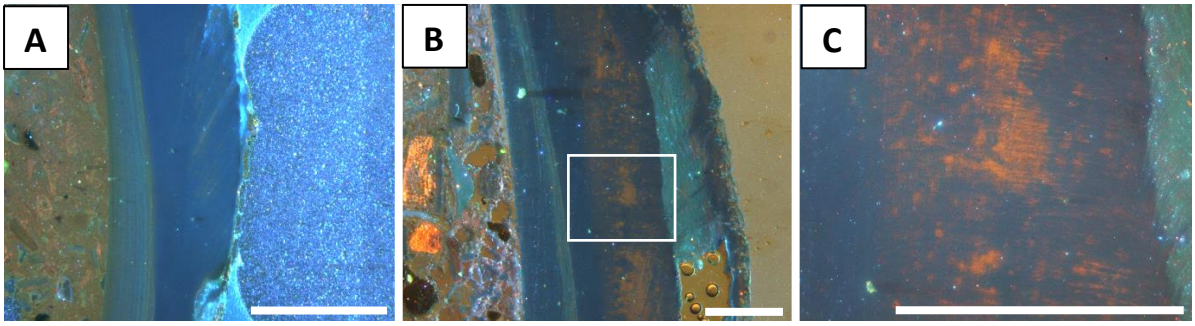

Figure 7

[Fig. 7 – for 2-column reproduction; colour required]

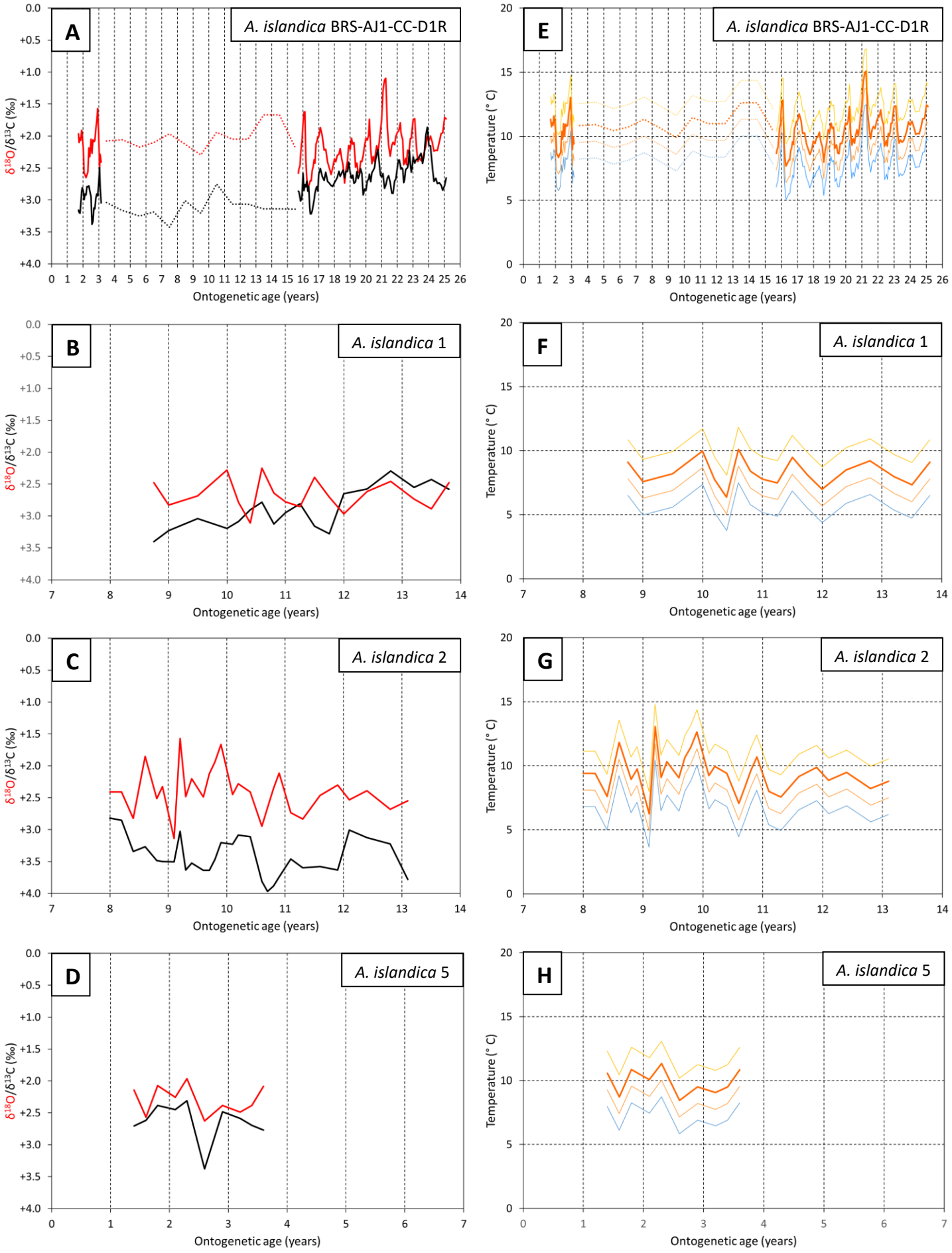

Figure 8

[Fig. 8 – for 2-column reproduction; colour required]

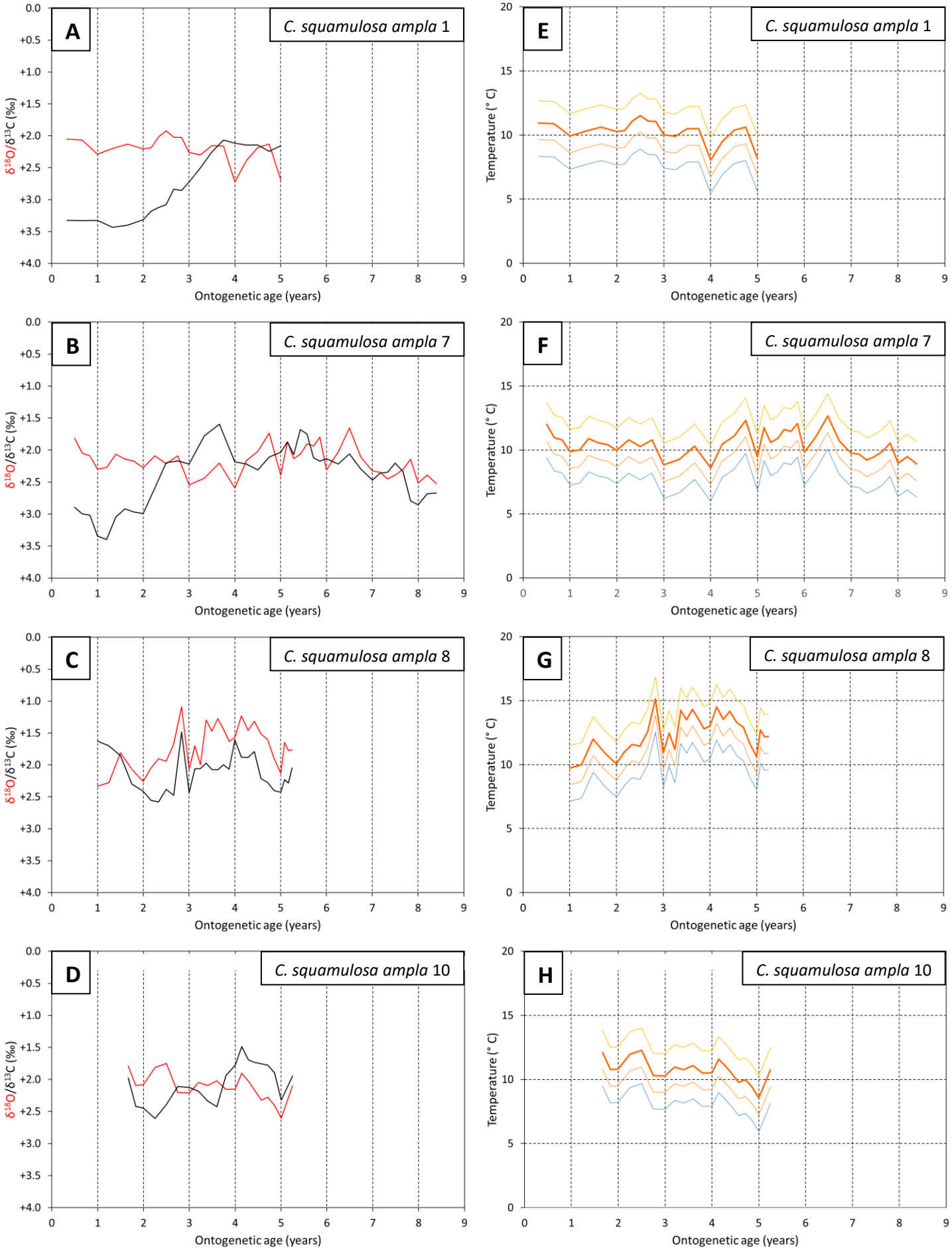

Figure 9

[Fig. 9 – for 2-column reproduction; colour required]

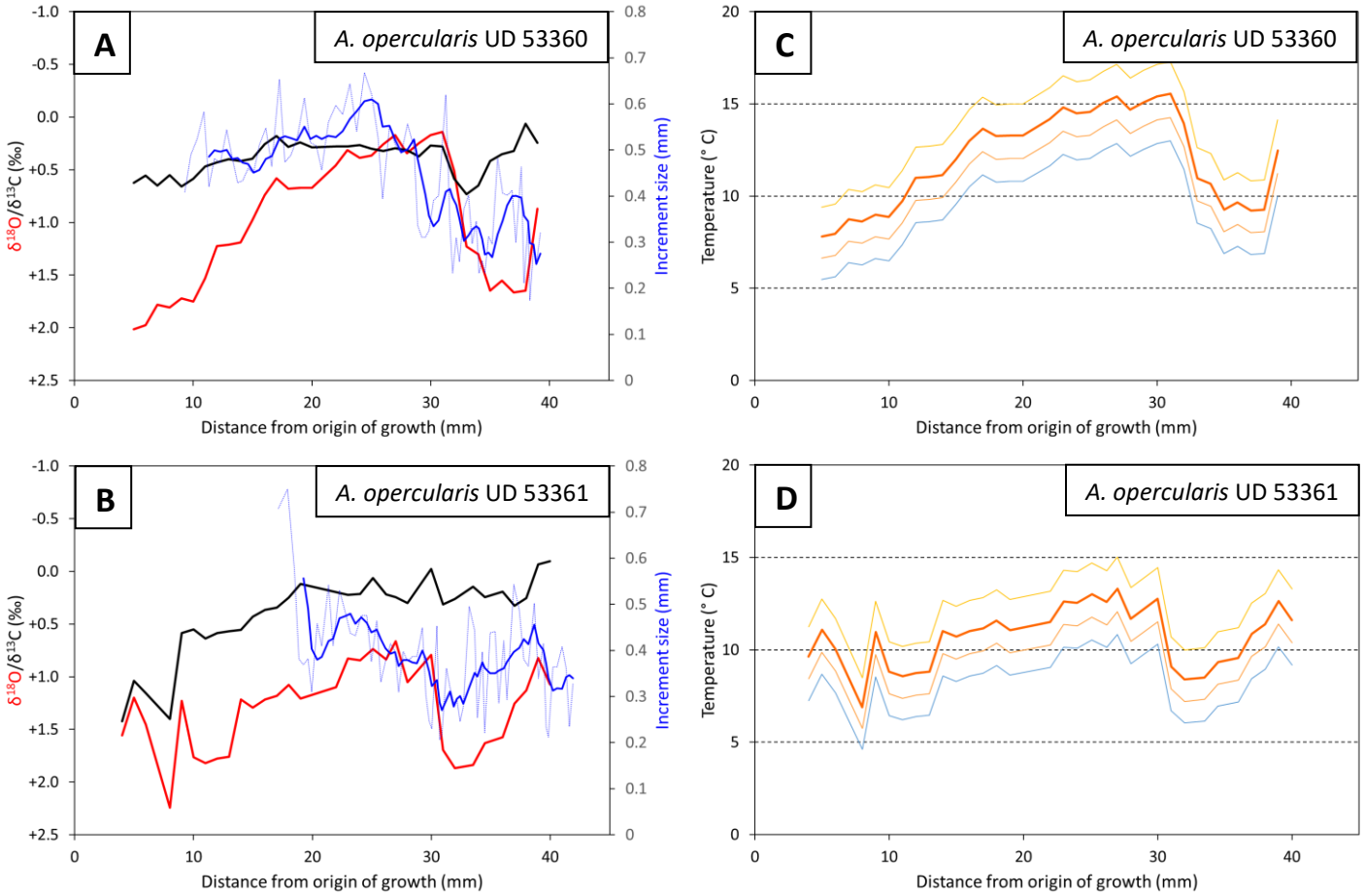

Figure 10

[Fig. 10 – for 2-column reproduction; colour required]

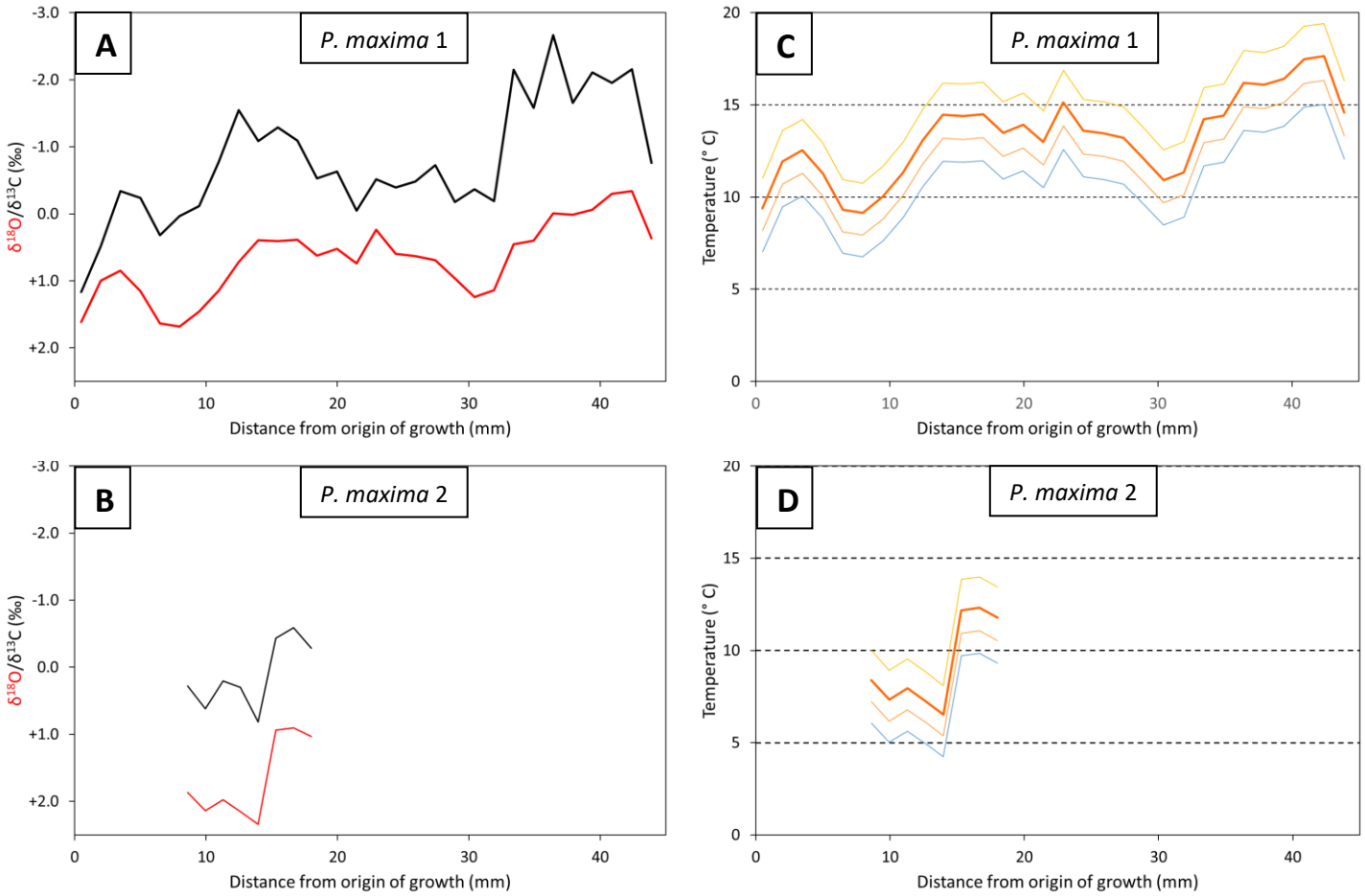

Figure 11

[Fig. 11 – for 2-column reproduction; colour required]

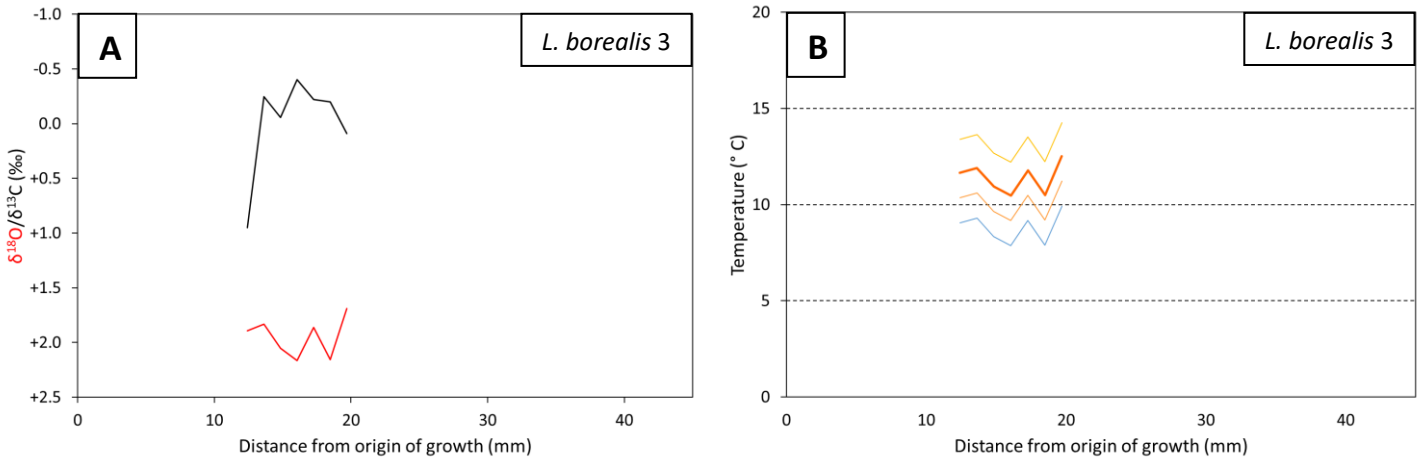

Figure 12

[Fig. 12 – for 1.5 or 2-column reproduction; colour required]

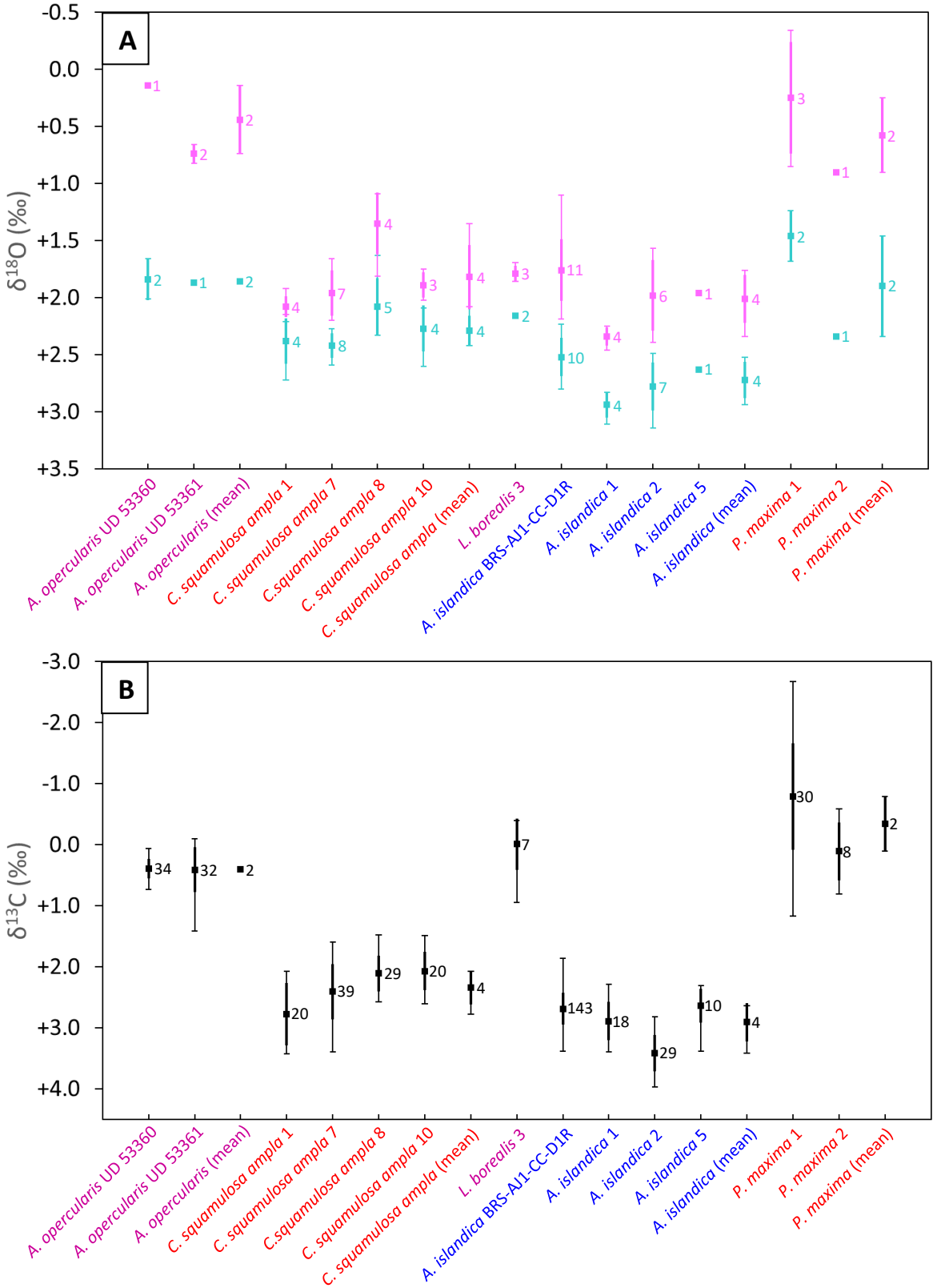

Figure 13

[Fig. 13 – for 1.5- or 2-column reproduction; colour required]

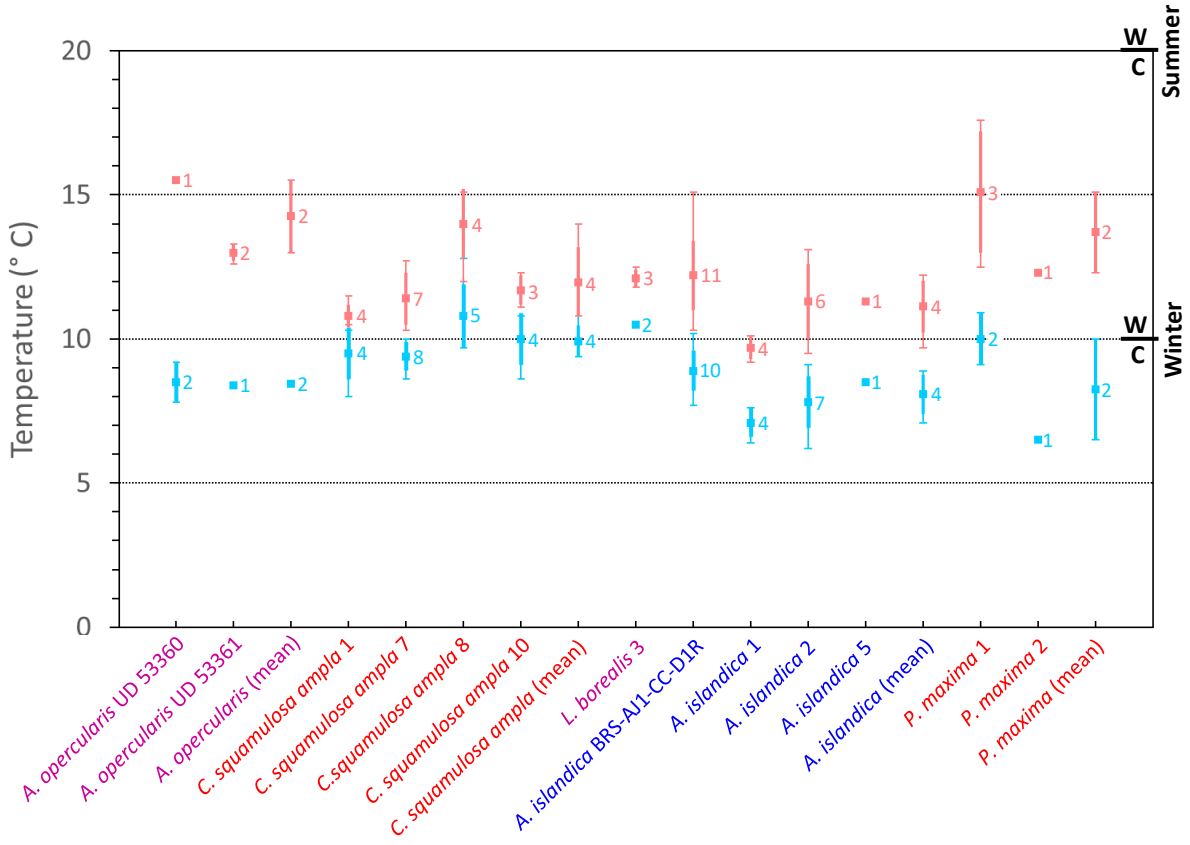

Figure 14

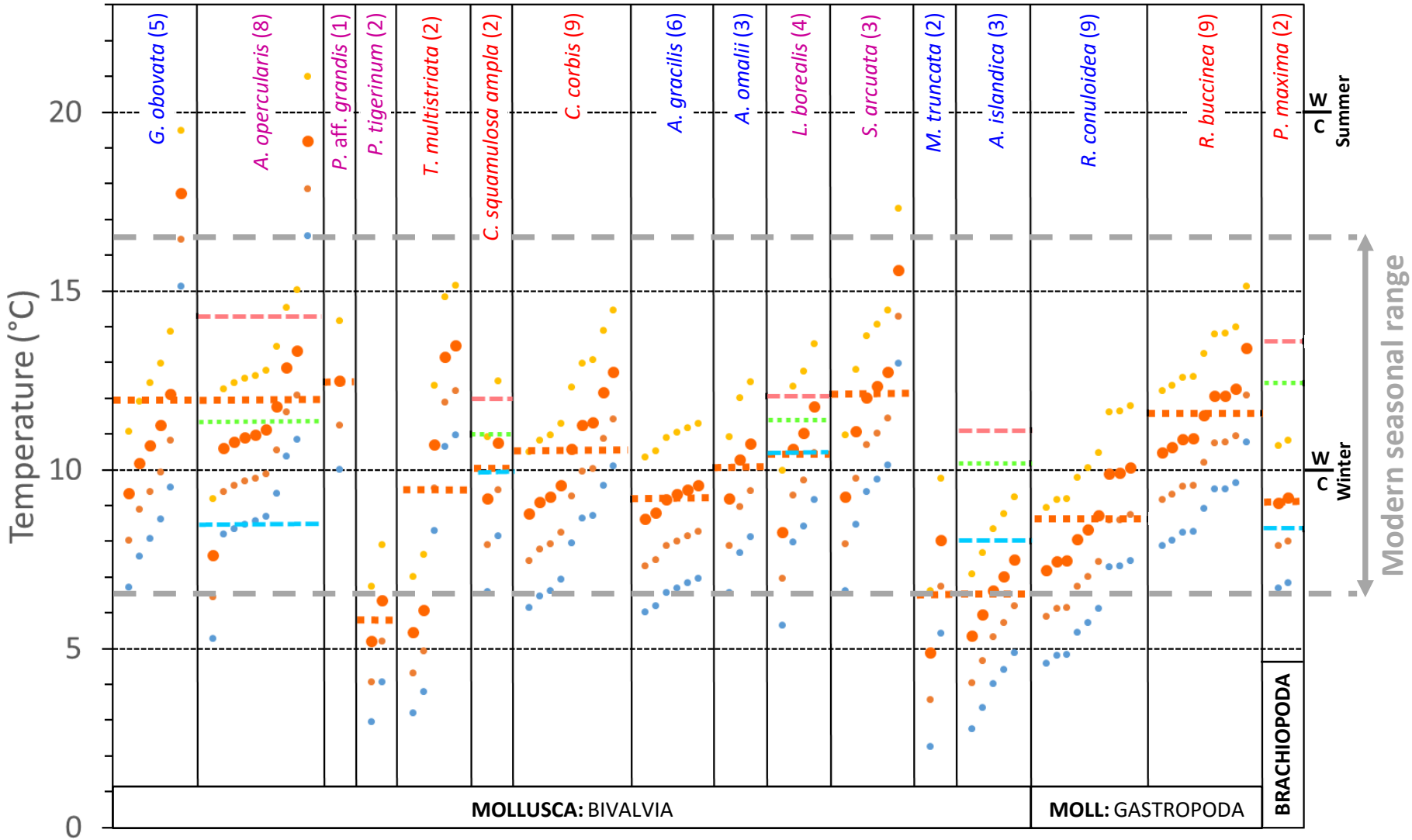

[Fig. 14 – for 2-column reproduction; colour required]

Supplementary Material A

Click here to download Background dataset for online publication only: Supplementary Material A - Vignols et al..xlsx

Supplementary Material B

Click here to download Background dataset for online publication only: Supplementary Material B - Vignols et al..docx